Reduced-order modeling of laminar-turbulent transition in large-eddy simulations

Philipp Hack

CENTER FOR TURBULENCE RESEARCH

Advanced Modeling and Simulation Seminar Series
NASA/Ames May 2019

Stability research at CTR

Flow separation

High-speed flows

Jet noise

Nonlinear stability

Atomization

Reduced-order modeling

<u>Flow separation reduces aerodynamic performance</u>

→ How can separation be delayed/avoided most effectively?

→ Most effective mechanism of separation delay exploits the gradients provided by the mean shear

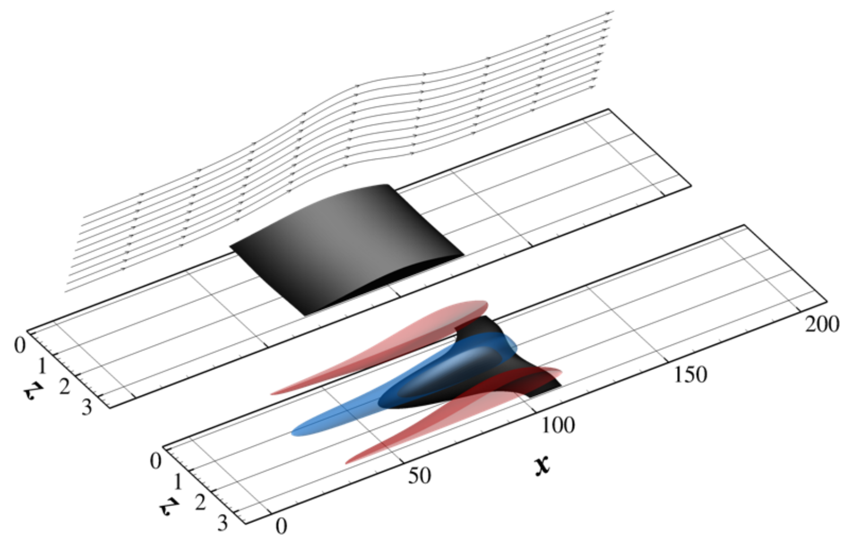

Stanford

Stability research at CTR

Flow separation | High-speed flows | Jet noise

Nonlinear stability | Atomization | Reduced-order modeling

<u>Transition to turbulence in hypersonic flows</u>

→ Breakdown to turbulence critically increases heat transfer

→ Adjoint-based receptivity and sensitivity analysis

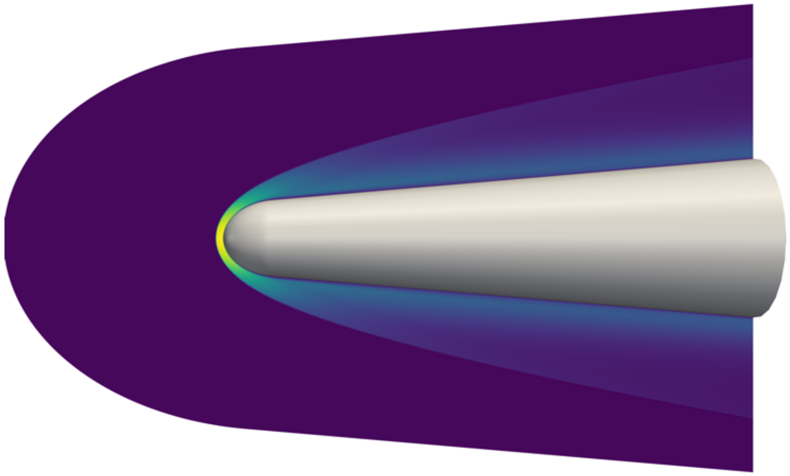

Stability research at CTR

Flow separation

High-speed flows

Jet noise

Nonlinear stability

Atomization

Reduced-order modeling

<u>Jet screech</u>

→ Critical phenomenon which reduces lifetime of jet engines

→ Global stability analysis to identify mechanism of jet screech

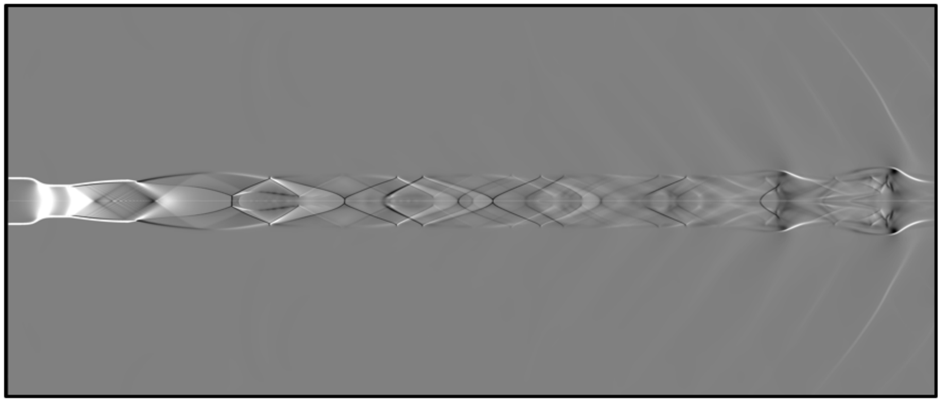

Stanford

Stability research at CTR

Flow separation | High-speed flows | Jet noise

Nonlinear stability | Atomization | Reduced-order modeling

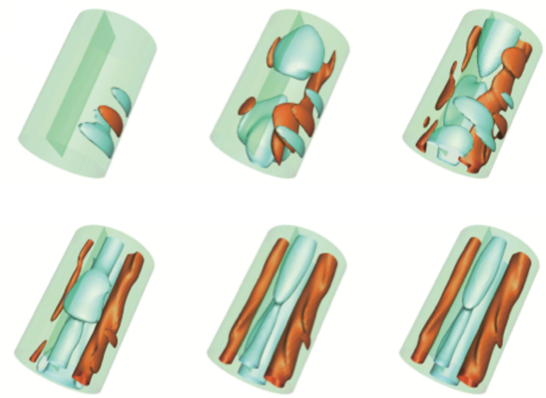

Nonlinear optimal disturbances

→ Classical linear stability theory valid in the limit of small perturbations

→ Breakdown to turbulence results from strong nonlinear interactions

Stability research at CTR

Flow separation | High-speed flows | Jet noise

Nonlinear stability | Atomization | Reduced-order modeling

<u>Fragmentation of liquid jets</u>

→ Effective atomization of liquid jets critical in many applications

→ Non-exponential mechanisms can lead to fragmentation

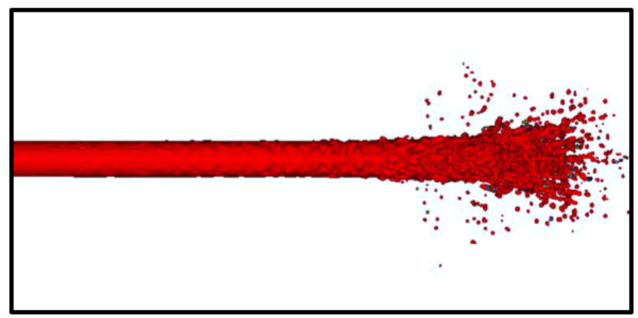

Stability research at CTR

Flow separation

High-speed flows

Jet noise

Nonlinear stability

Atomization

Reduced-order modeling

<u>Reduced-order modeling of transitional flows:</u>

→ Accurate yet efficient model of transition to turbulence

→ Physics-based formulation without tunable parameters

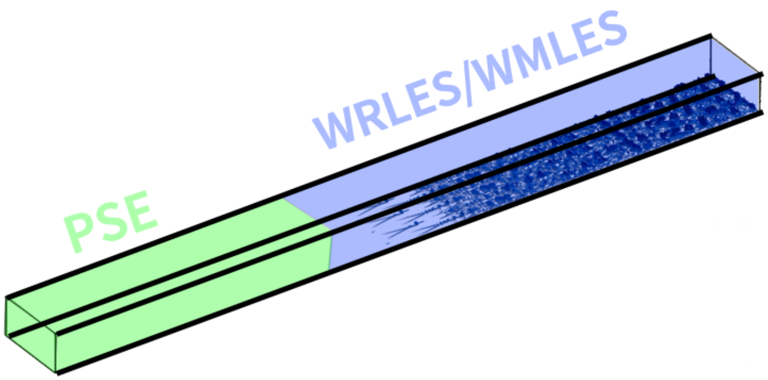

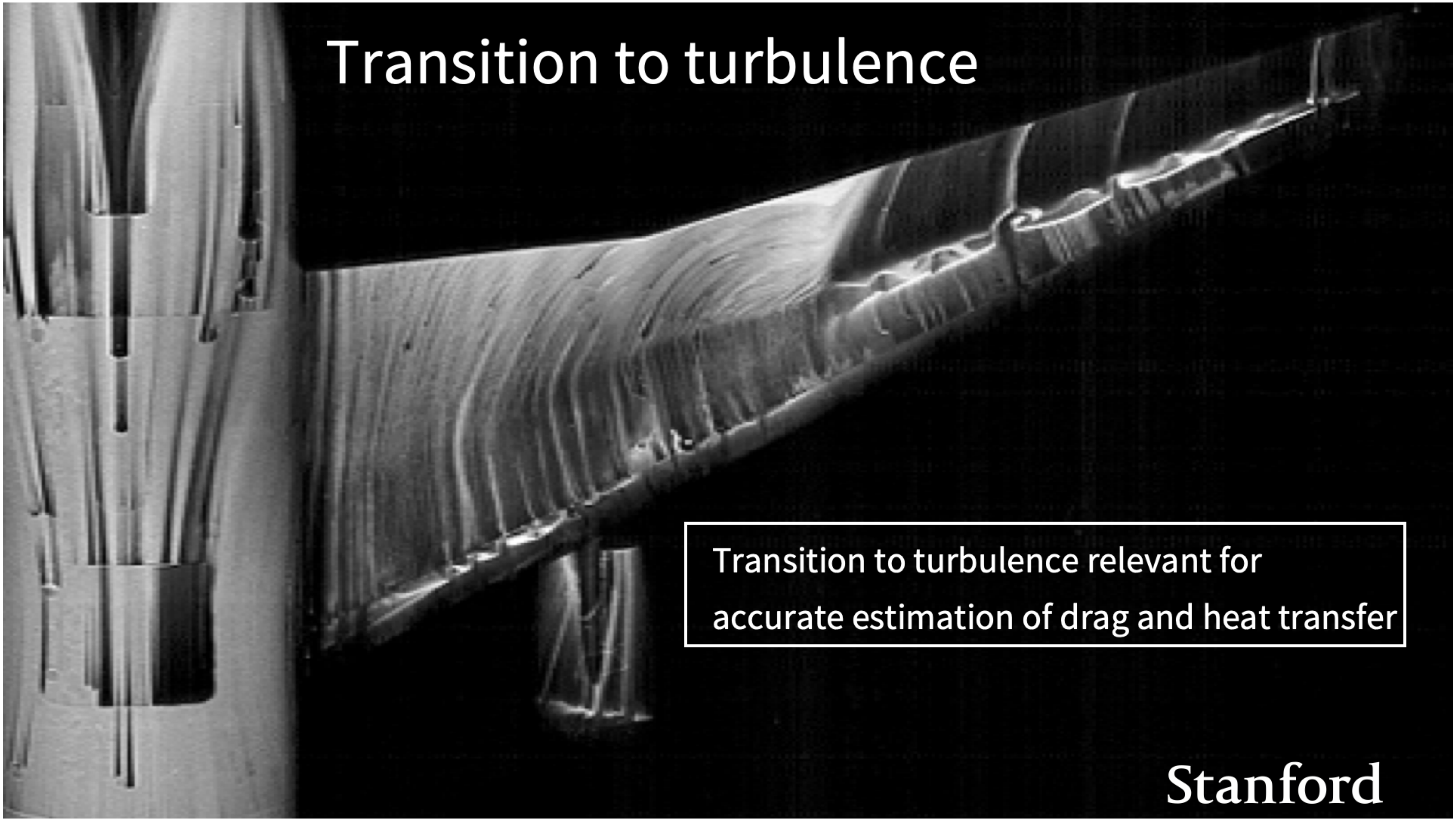
Transition to turbulence
Transition to turbulence relevant for
accurate estimation of drag and heat transfer
Stanford

Transition to turbulence

LES of transitional boundary layer

Park 2014

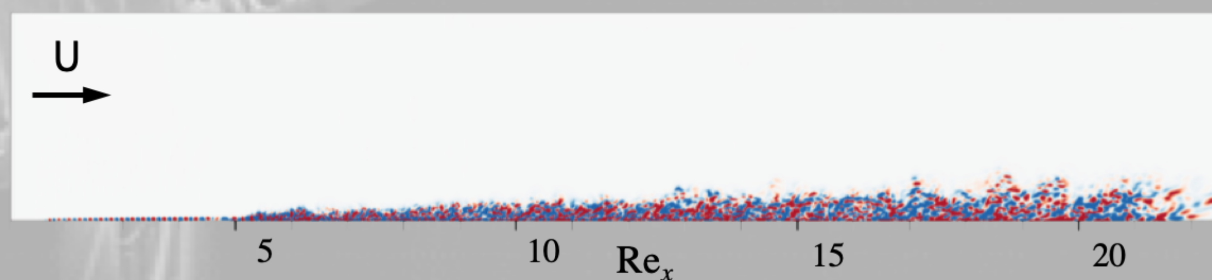

"In order to capture the correct streamwise growth of the disturbance waves, fine resolution is needed in the laminar region (otherwise the flow stays laminar)."

Transition to turbulence

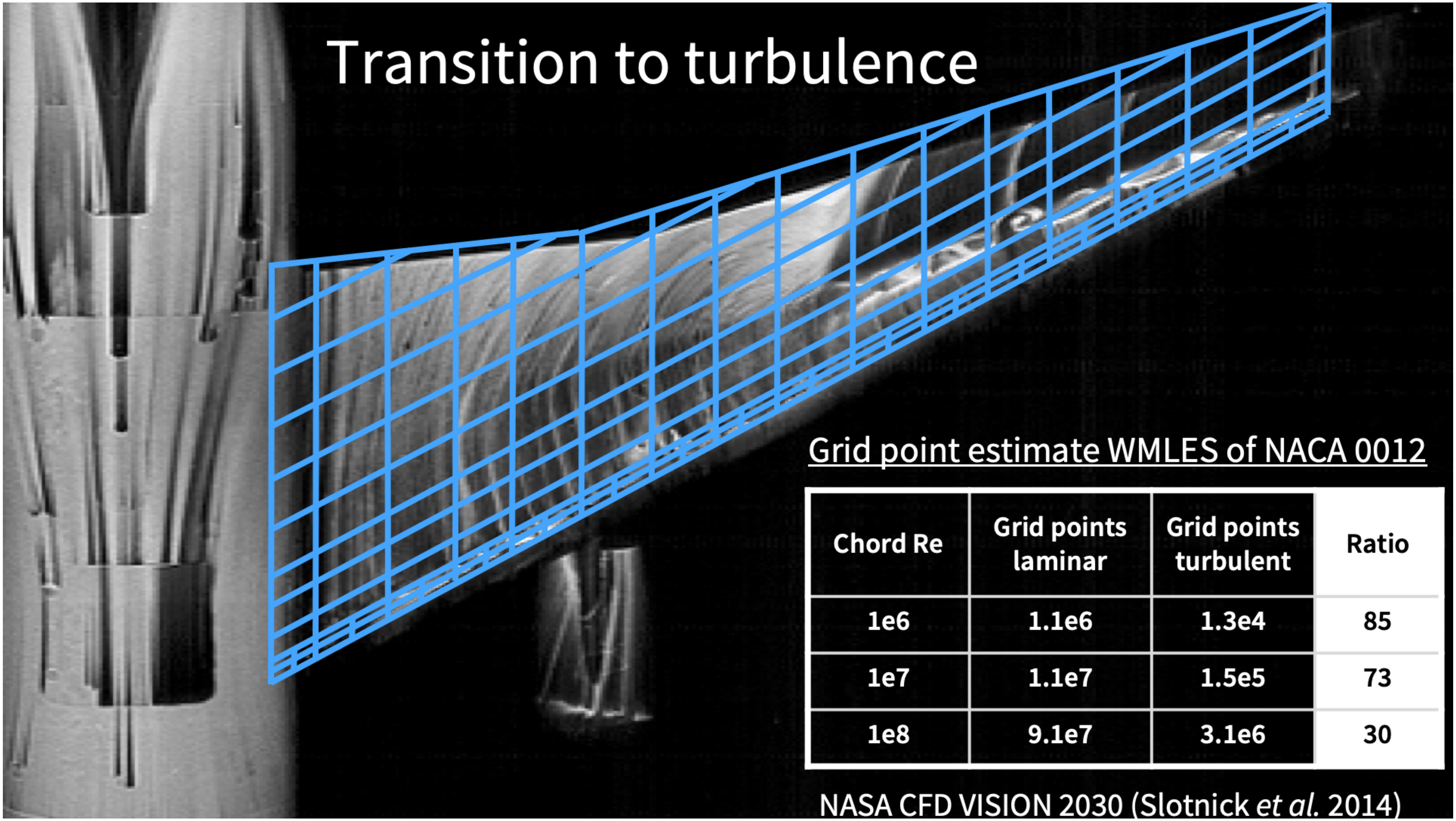

Grid point estimate WMLES of NACA 0012

Chord Re	Grid points laminar	Grid points turbulent	Ratio
1e6	1.1e6	1.3e4	85
1e7	1.1e7	1.5e5	73
1e8	9.1e7	3.1e6	30

NASA CFD VISION 2030 (Slotnick *et al.* 2014)

Transition to turbulence

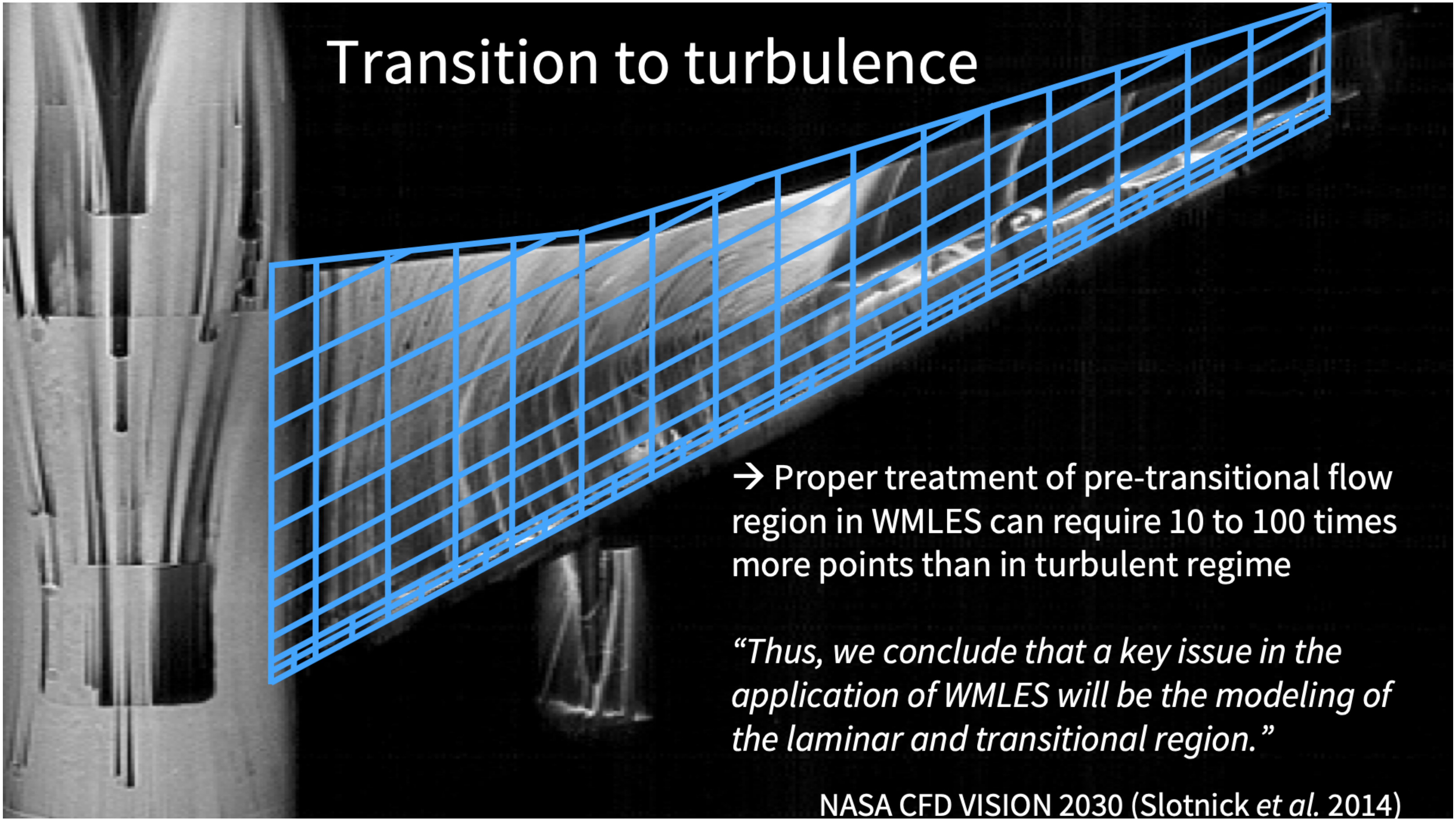

→ Proper treatment of pre-transitional flow region in WMLES can require 10 to 100 times more points than in turbulent regime

"Thus, we conclude that a key issue in the application of WMLES will be the modeling of the laminar and transitional region."

NASA CFD VISION 2030 (Slotnick *et al.* 2014)

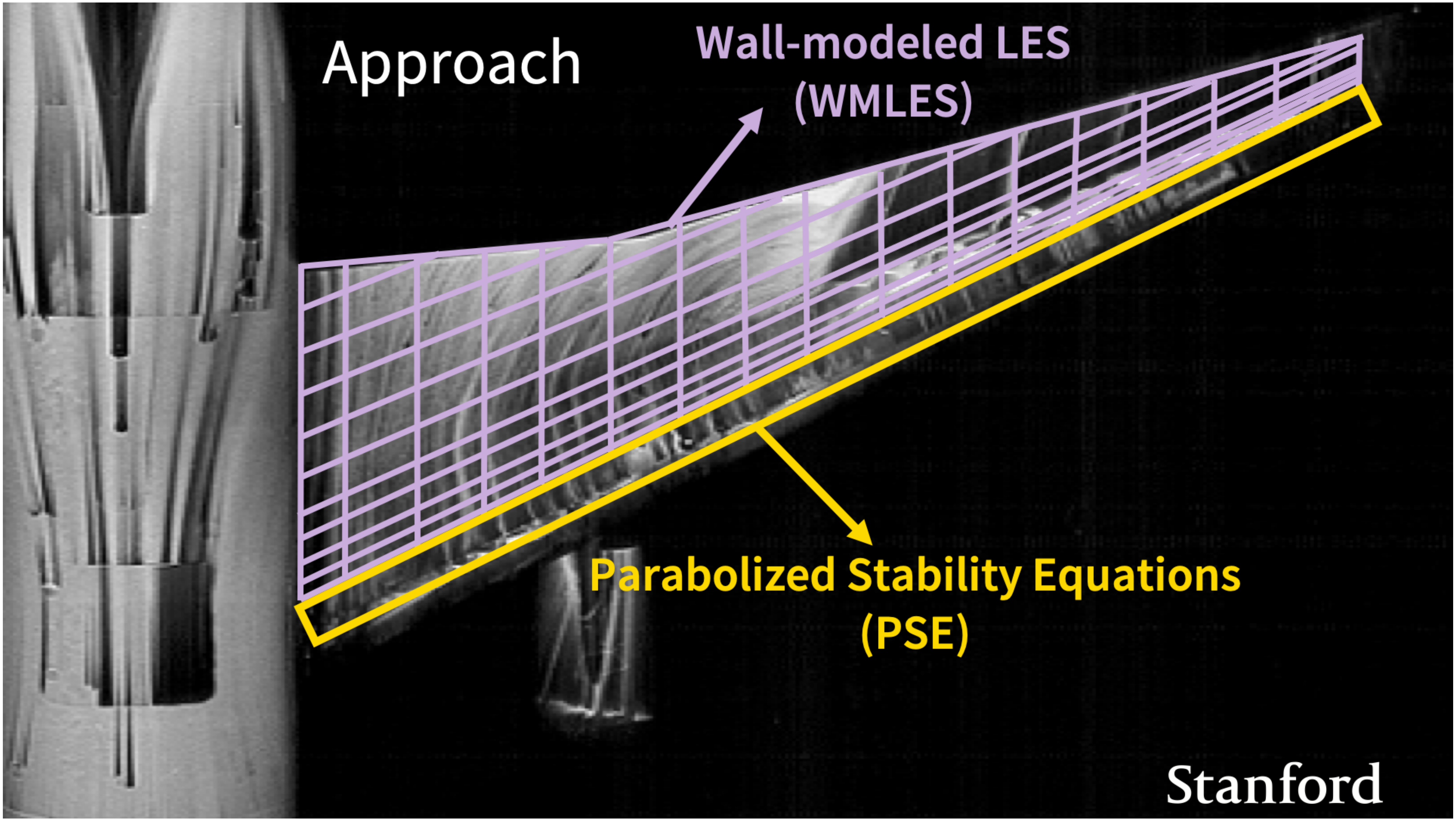
Approach
Wall-modeled LES
(WMLES)
Parabolized Stability Equations
(PSE)
Stanford

Stages of the transition process

Natural transition in boundary layer

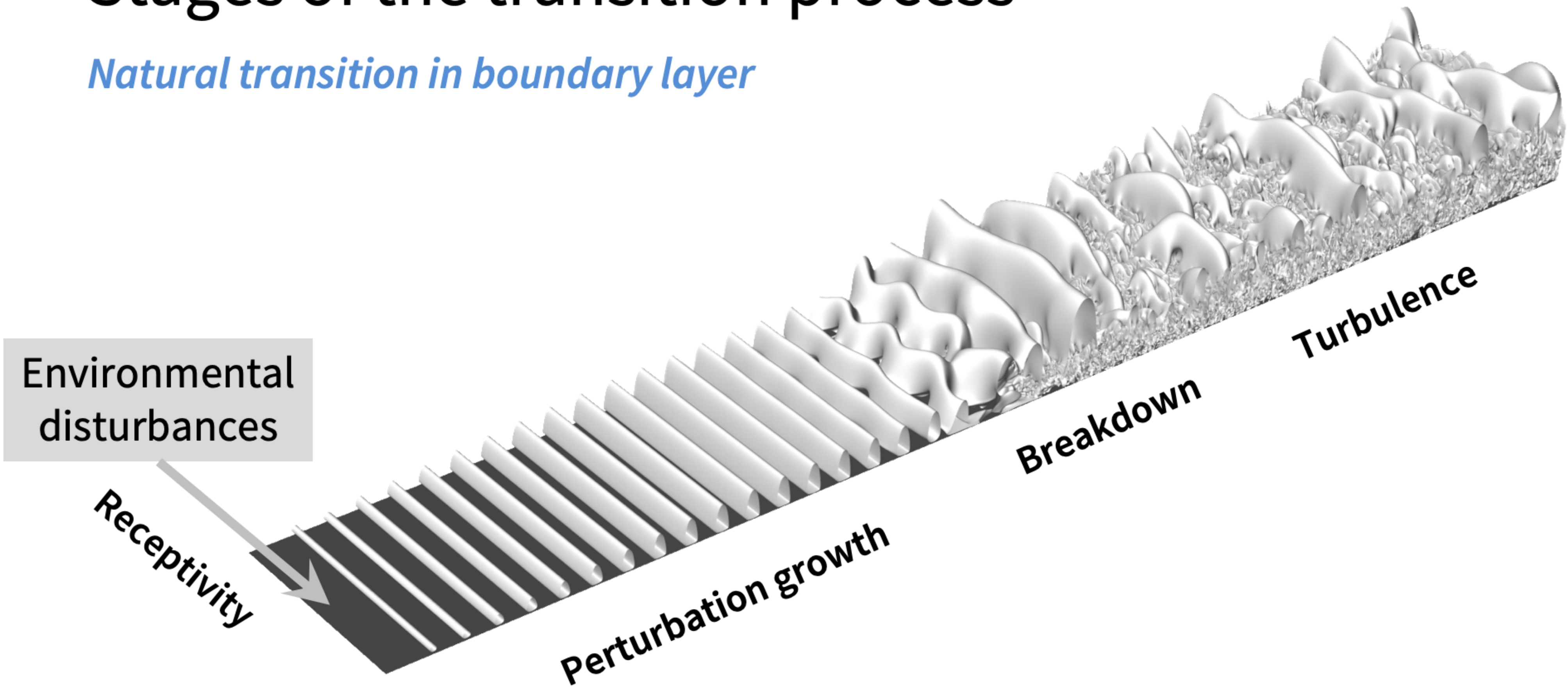

Transition scenarios

NATURAL

- Low levels of external disturbances
- Exponential amplification of primary disturbances (TS waves)
- Classical configurations: H/K-type (Herbert 1988, Kachanov 1984)

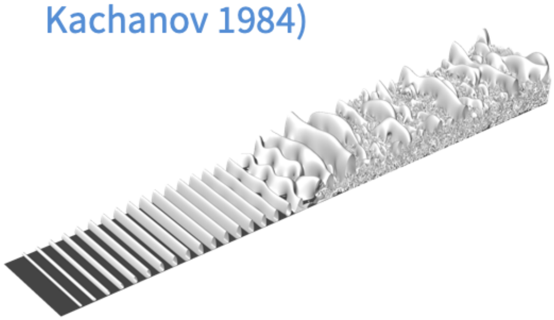

BYPASS

- Moderate levels of external disturbances
- Algebraic amplification of primary disturbances (streaks)
- Exponential secondary instability

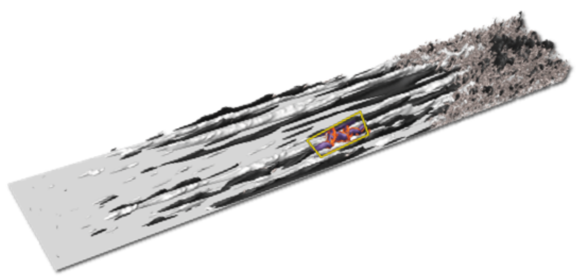

CROSSFLOW

- Inflectional (exponential) primary disturbance
- Rapid breakdown to turbulence

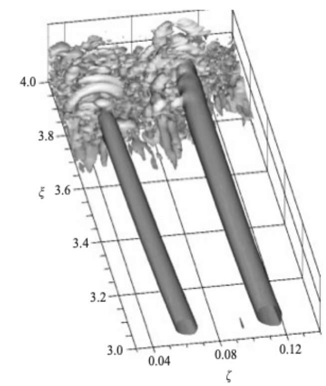

Transition scenarios

NATURAL	BYPASS	CROSSFLOW
• Low levels of external disturbances • Exponential amplification of primary disturbances (TS waves) • Classical configurations: H/K-type (Herbert 1988, Kachanov 1984)	• Moderate levels of external disturbances • Algebraic amplification of primary disturbances (streaks) • Exponential secondary instability	• Inflectional (exponential) primary disturbance • Rapid breakdown to turbulence
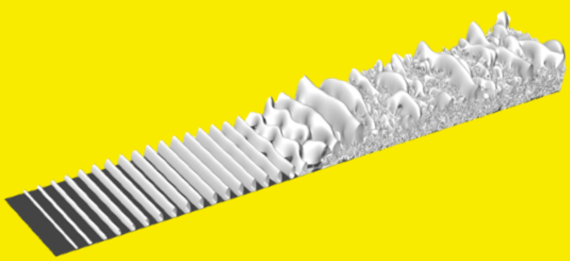	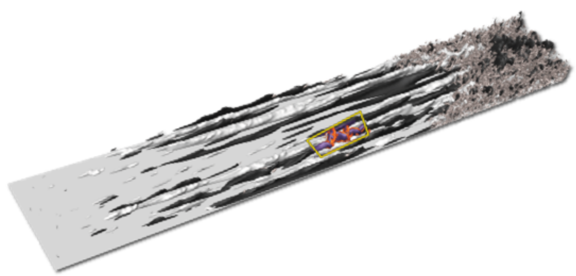	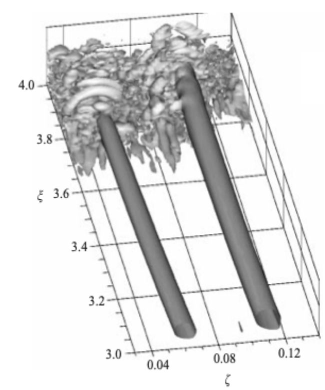

Parabolized Stability Equations (Herbert 1992)

Laminar pre-transitional boundary layer

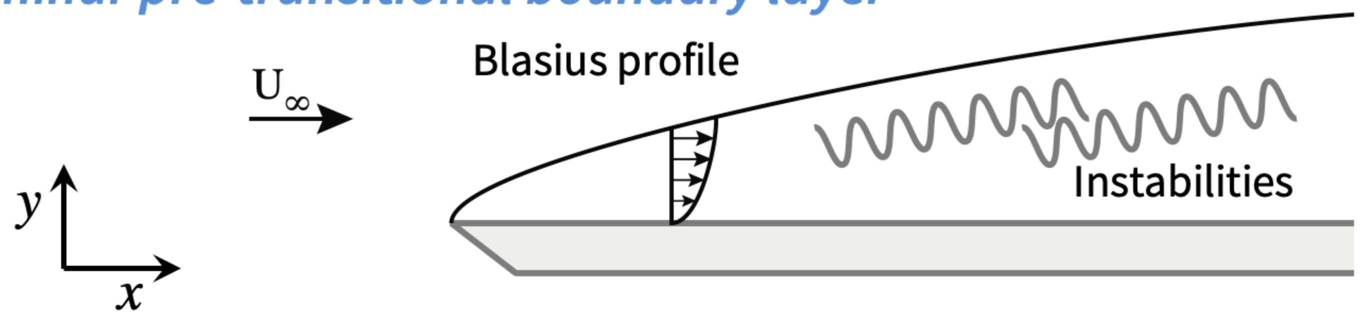

Parabolized Stability Equations (Herbert 1992)

Sufficient distance to leading edge

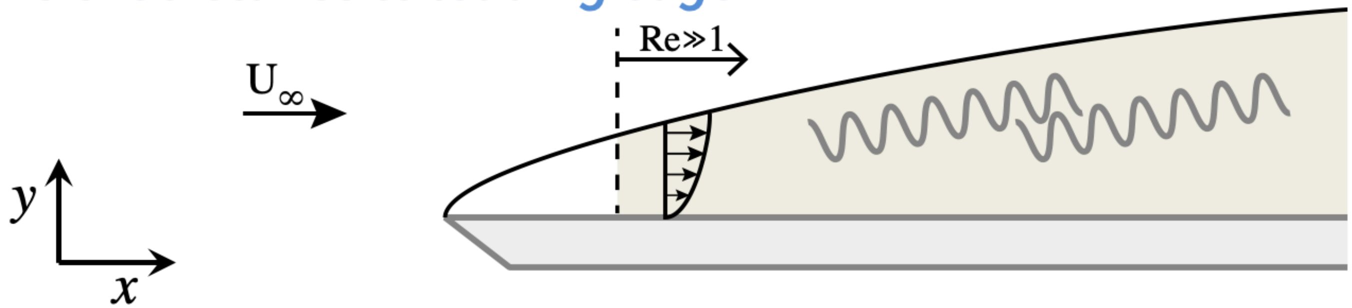

Parabolized Stability Equations

Separation of the state

Base

$$\bar{\boldsymbol{q}}\left(x,y\right)=\left(\bar{u},\bar{v},\bar{w},\bar{p}\right)^{\mathsf{T}}$$

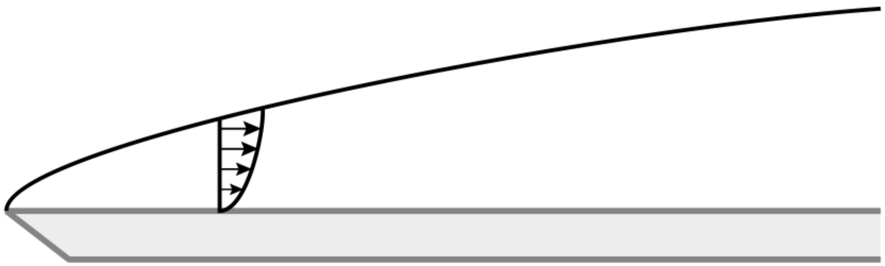

+

Perturbations

$$\boldsymbol{q}'\left(x,y,z,t\right)=\left(u',v',w',p'\right)^{\mathsf{T}}$$

Parabolized Stability Equations

Separation of the perturbations

Base

$$\bar{\boldsymbol{q}}\,(x,y) = (\bar{u},\bar{v},\bar{w},\bar{p})^{\mathsf{T}}$$

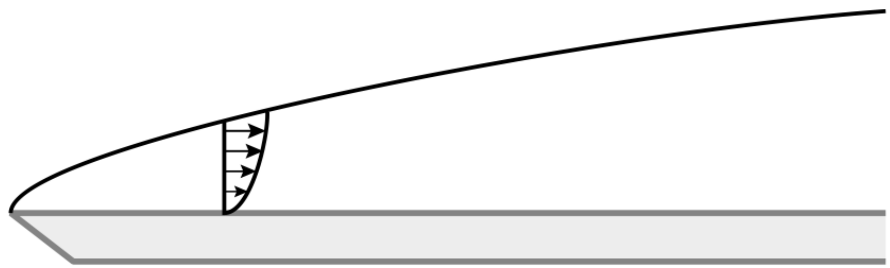

Perturbations

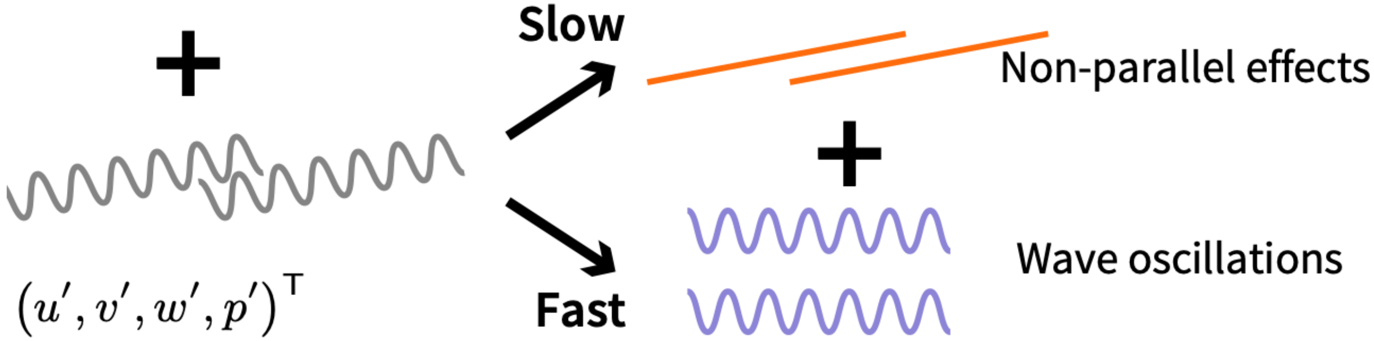

$$\boldsymbol{q}'\,(x,y,z,t) = (u',v',w',p')^{\mathsf{T}}$$

Parabolized Stability Equations

Separation of the perturbations

Base

$$\bar{\boldsymbol{q}}\,(x,y) = (\bar{u},\bar{v},\bar{w},\bar{p})^{\mathsf{T}}$$

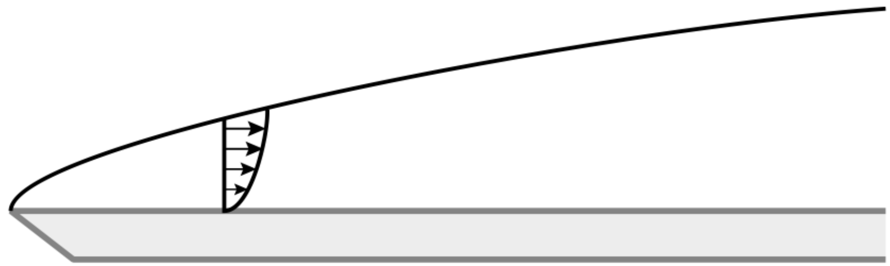

+

Perturbations

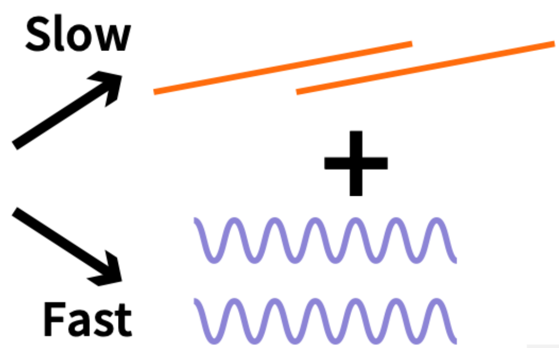

$$\boldsymbol{q}'\,(x,y,z,t) = (u',v',w',p')^{\mathsf{T}}$$

Ansatz: $$\boldsymbol{q}'\,(x,y,z,t) = \widehat{\boldsymbol{q}}\,(x,y)\exp\left(\mathrm{i}\,(\beta z + \omega t)\right)\exp\left(\mathrm{i}\int_{x_0}^{x}\alpha\,(\xi)\,\mathrm{d}\xi\right)$$

Subject to

$$\frac{\partial}{\partial x}\int_0^{\infty}\widehat{\boldsymbol{q}}^{H}\widehat{\boldsymbol{q}}\,\mathrm{d}y = 0$$

Parabolized Stability Equations

Derivation

$$\boldsymbol{q}'(x,y,z,t) = \widehat{\boldsymbol{q}}(x,y)\exp\left(\mathrm{i}\left(\beta z + \omega t\right)\right)\exp\left(\mathrm{i}\int_{x_0}^{x}\alpha(\xi)\,\mathrm{d}\xi\right)$$

$\downarrow$

$\boxed{\text{Navier-Stokes}}$

$\downarrow$

$\boxed{\mathcal{O}\left(Re^{-1}\right)}$

$\downarrow$

Parabolized Stability Equations (PSE)

Parabolized Stability Equations

For the n^{th} harmonic in span and the m^{th} harmonic in time:

$$\mathbf{A}\hat{\mathbf{q}}_{n,m} + \mathbf{B}\frac{\partial \hat{\mathbf{q}}_{n,m}}{\partial y} + \mathbf{C}\frac{\partial^2 \hat{\mathbf{q}}_{n,m}}{\partial y^2} + \mathbf{D}\frac{\partial \hat{\mathbf{q}}_{n,m}}{\partial x} = \boxed{\hat{\mathbf{F}}_{n,m}}$$

Nonlinear coupling of harmonics

with

$$\mathbf{A} = \begin{bmatrix} r + \frac{\partial U}{\partial x} & \frac{\partial U}{\partial y} & 0 & i\alpha \\ 0 & r + \frac{\partial V}{\partial y} & 0 & 0 \\ \frac{\partial W}{\partial x} & \frac{\partial W}{\partial y} & r & in\beta \\ i\alpha & 0 & in\beta & 0 \end{bmatrix}, \qquad \mathbf{B} = \begin{bmatrix} V & 0 & 0 & 0 \\ 0 & V & 0 & 1 \\ 0 & 0 & V & 0 \\ 0 & 1 & 0 & 0 \end{bmatrix},$$

$$\mathbf{C} = \begin{bmatrix} -\frac{1}{Re} & 0 & 0 & 0 \\ 0 & -\frac{1}{Re} & 0 & 0 \\ 0 & 0 & -\frac{1}{Re} & 0 \\ 0 & 0 & 0 & 0 \end{bmatrix}, \qquad \mathbf{D} = \begin{bmatrix} U & 0 & 0 & 1 \\ 0 & U & 0 & 0 \\ 0 & 0 & U & 0 \\ 1 & 0 & 0 & 0 \end{bmatrix},$$

where $r = -im\omega + i\alpha_{n,m}U + in\beta W + \frac{1}{Re}(\alpha_{n,m}^2 + n^2\beta^2)$

Stanford

Parabolized Stability Equations

Comparison to CFD

Instability wave

CFD

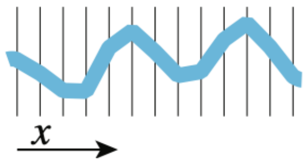

Wave represented
on discrete grid

$$\Delta x < \lambda$$

Parabolized Stability Equations

Comparison to CFD

Instability wave

CFD

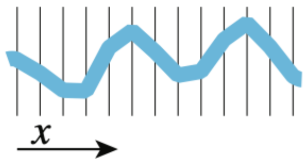

Wave represented on discrete grid

$$\Delta x < \lambda$$

PSE

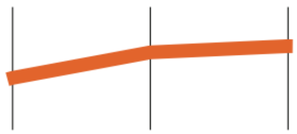

$$\hat{\boldsymbol{q}}(x, y)$$

$$\times$$

$$\exp\left(\mathrm{i}\int_{x_0}^{x} \alpha(\xi)\,\mathrm{d}\xi\right)$$

→ Only the slow-changing part requires support on discrete grid

→ Significantly larger Δx

Parabolized Stability Equations

Comparison to CFD

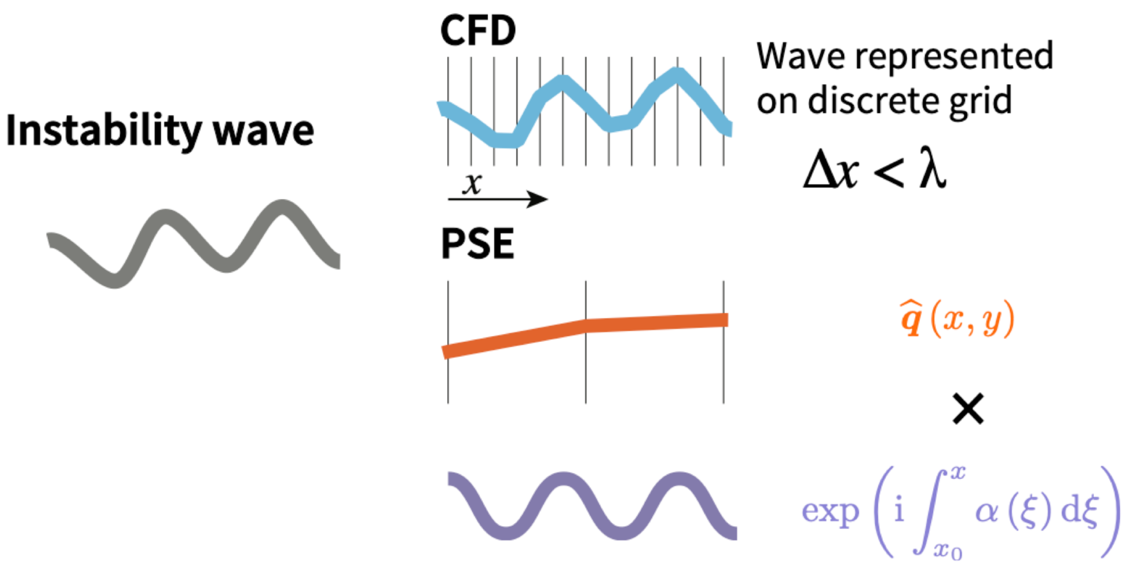

	CFD	PSE
Time	Integration	Limited harmonic expansion
Span	FD/FV/Spectral	Limited harmonic expansion
Normal	FD/FV/Spectral	Spectral
Pressure	2D/3D ellipticity	1D ellipticity

→ PSE offer substantial computational savings

Parabolized Stability Equations

Capabilities

Compatible with

- Growth of exponential instabilities
- Nonparallel effects
  (boundary layer growth)
- Nonlinear effects (mode interaction)
- Three-dimensional flows (swept wings)
- Moderate surface curvature (attached flow)
- Moderate pressure gradient

Incompatible with

- Unsteady flows
- Flows at low Re, including leading edges
- Separation/recirculation
- Turbulence, including local spots

Numerical experiments

- Direct Numerical Simulation
- Zero-pressure-gradient flat-plate boundary layer
- H-type natural transition (Herbert 1988)

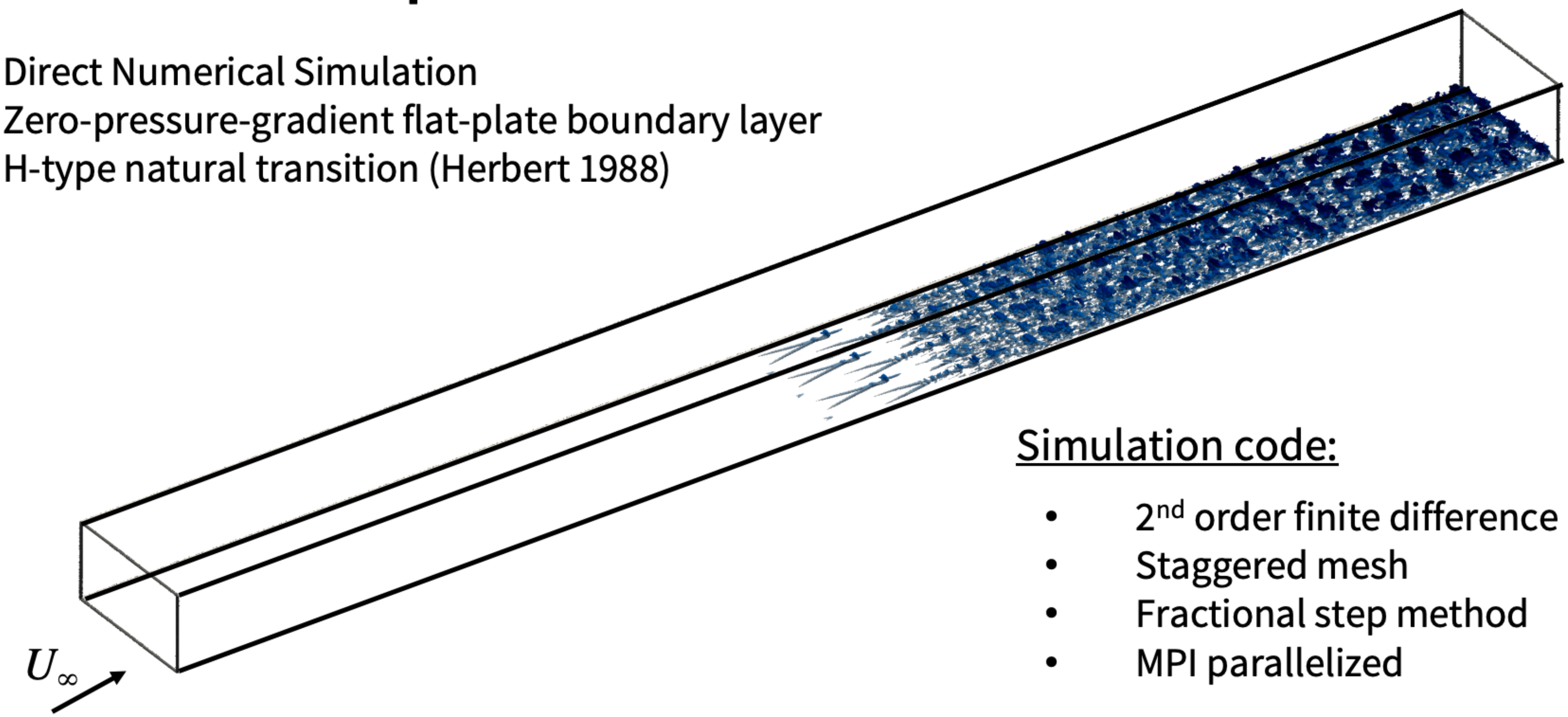

Simulation code:

- 2^{nd} order finite difference
- Staggered mesh
- Fractional step method
- MPI parallelized

Lozano-Durán, Hack & Moin, Phys. Rev. Fluids (2018)

Numerical experiments

- Direct Numerical Simulation
- Zero-pressure-gradient flat-plate boundary layer
- H-type natural transition (Herbert 1988)

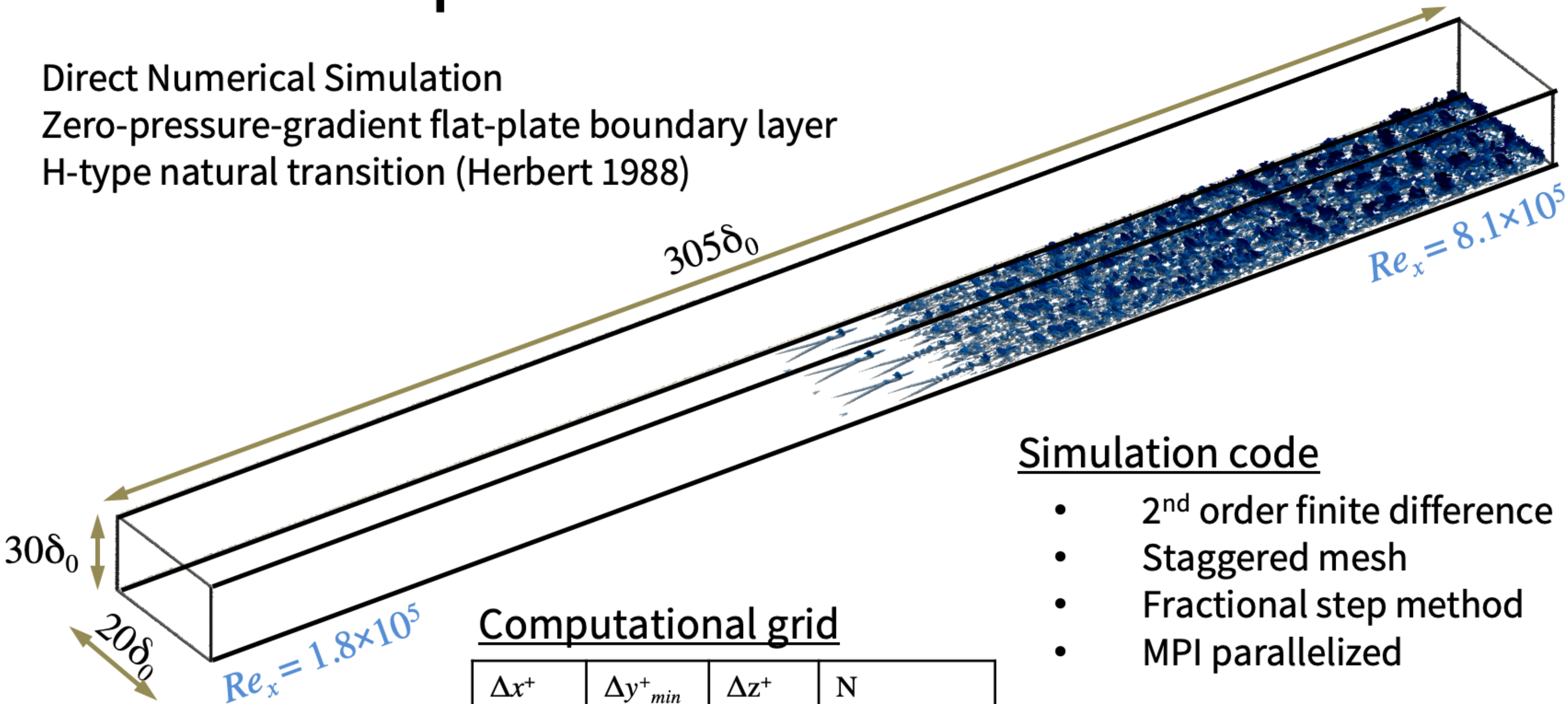

Simulation code

- 2nd order finite difference
- Staggered mesh
- Fractional step method
- MPI parallelized

Computational grid

Δx^+	Δy^+_{min}	Δz^+	N
7.2	0.3	5.1	250×10^6

Numerical experiments

- Direct Numerical Simulation
- Zero-pressure-gradient flat-plate boundary layer
- H-type natural transition (Herbert 1988)

Boundary conditions

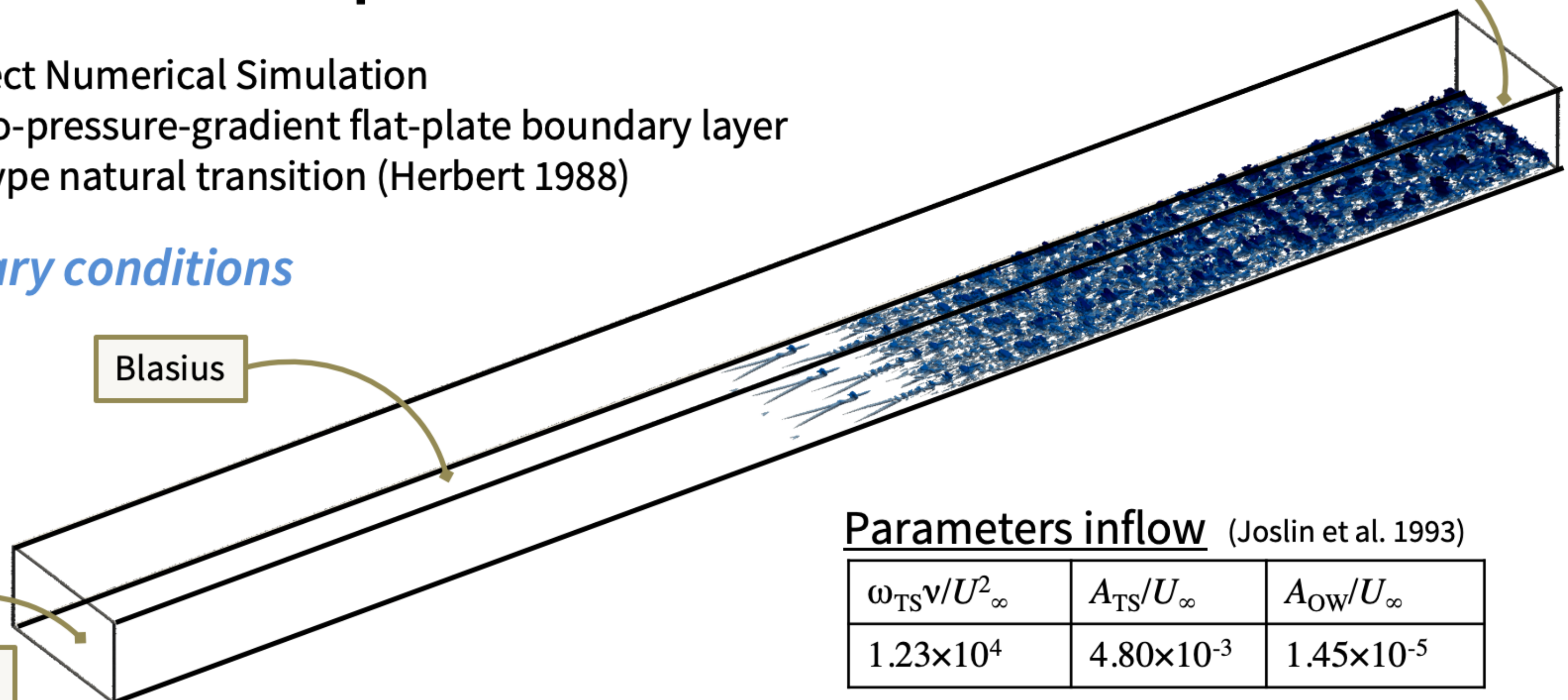

<u>Parameters inflow</u> (Joslin et al. 1993)

$\omega_{TS}\nu/U^2_\infty$	A_{TS}/U_∞	A_{OW}/U_∞
1.23×10^4	4.80×10^{-3}	1.45×10^{-5}

Lozano-Durán, Hack & Moin, Phys. Rev. Fluids (2018)

Numerical experiments

Considered setups

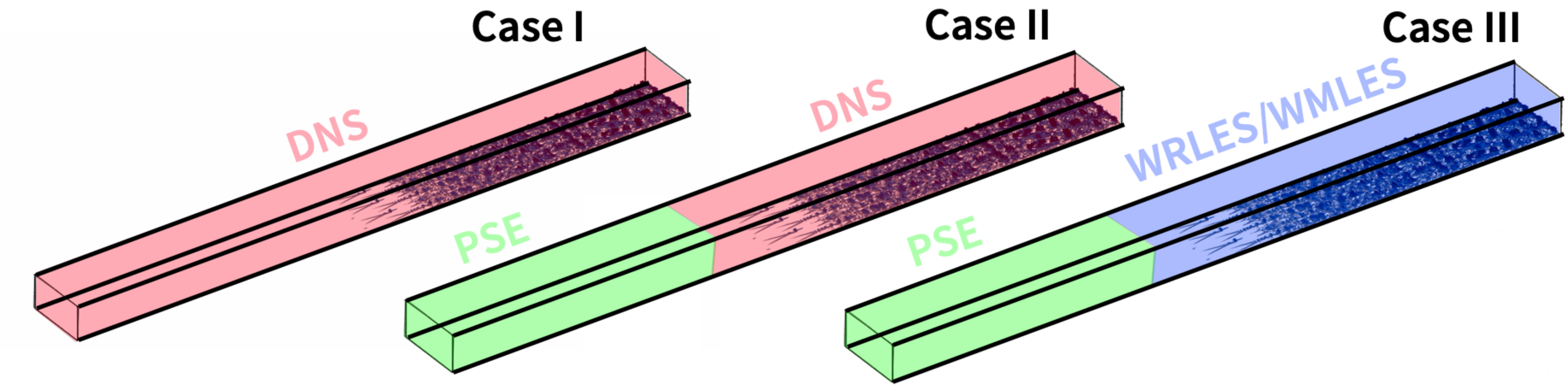

Numerical experiments

Considered setups

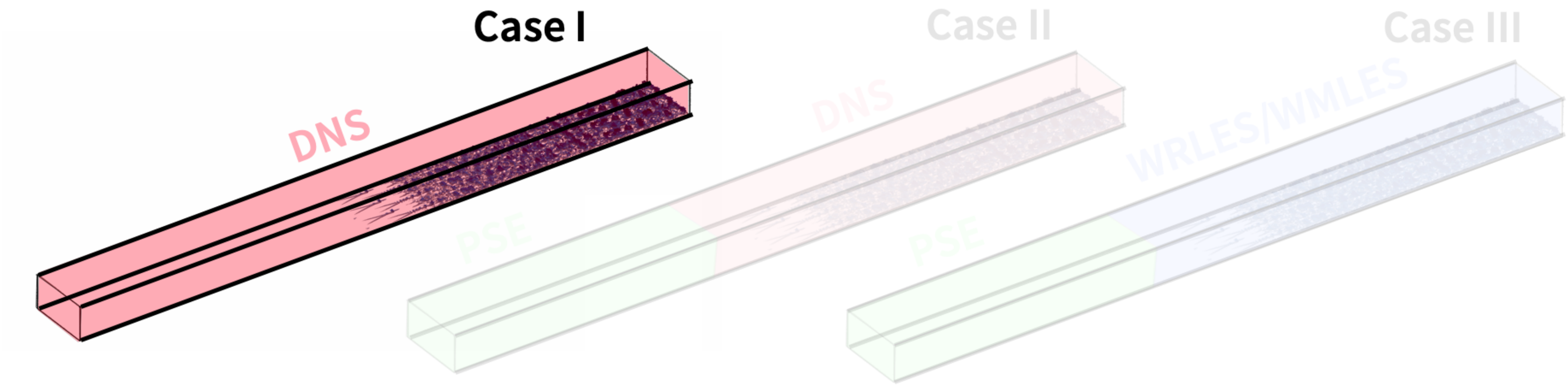

DNS

<u>Grid points</u>

Pre-transitional:	100M
Transitional+turbulent:	150M

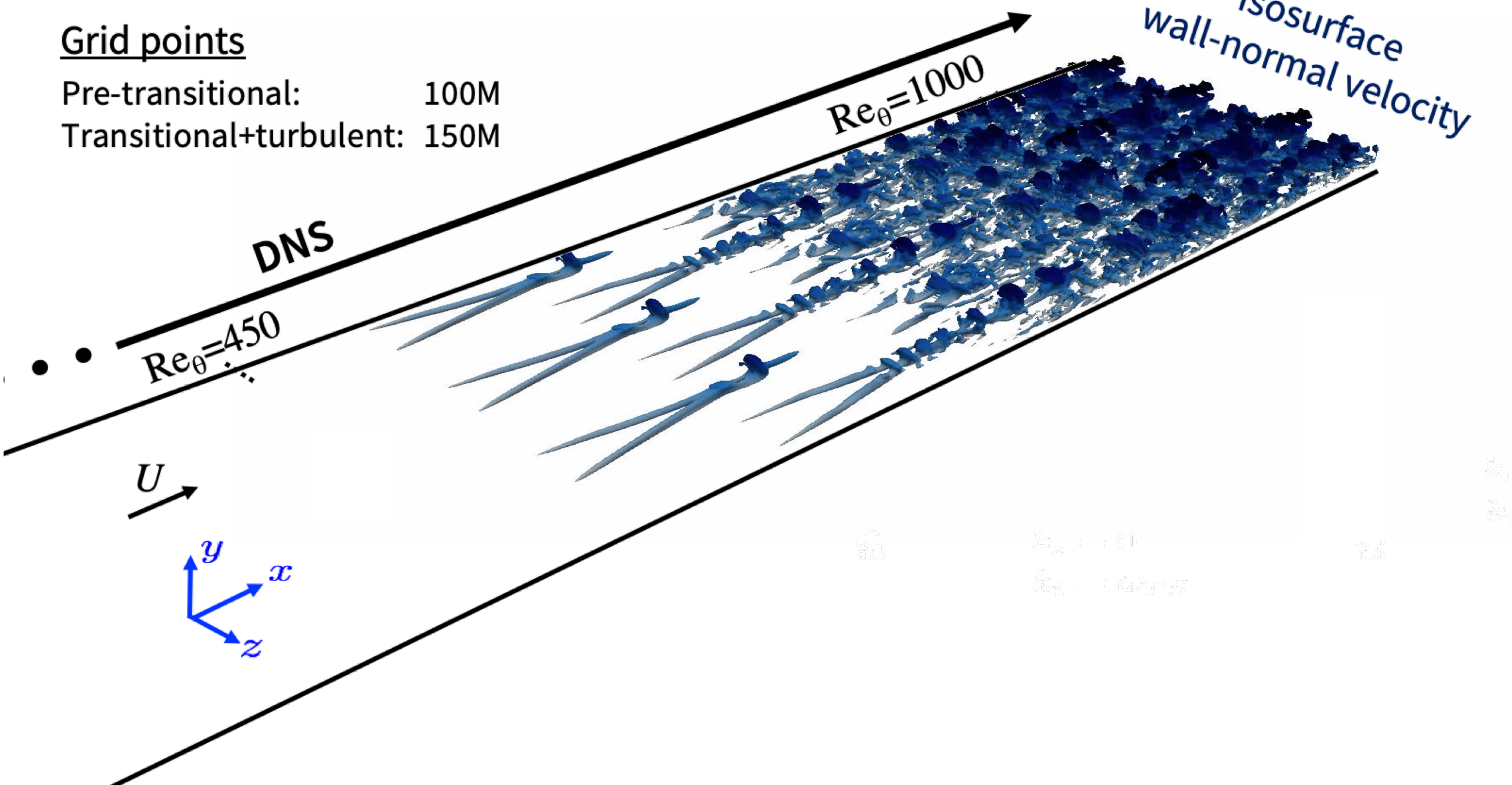

DNS

<u>Grid points</u>

Pre-transitional:	100M
Transitional+turbulent:	150M

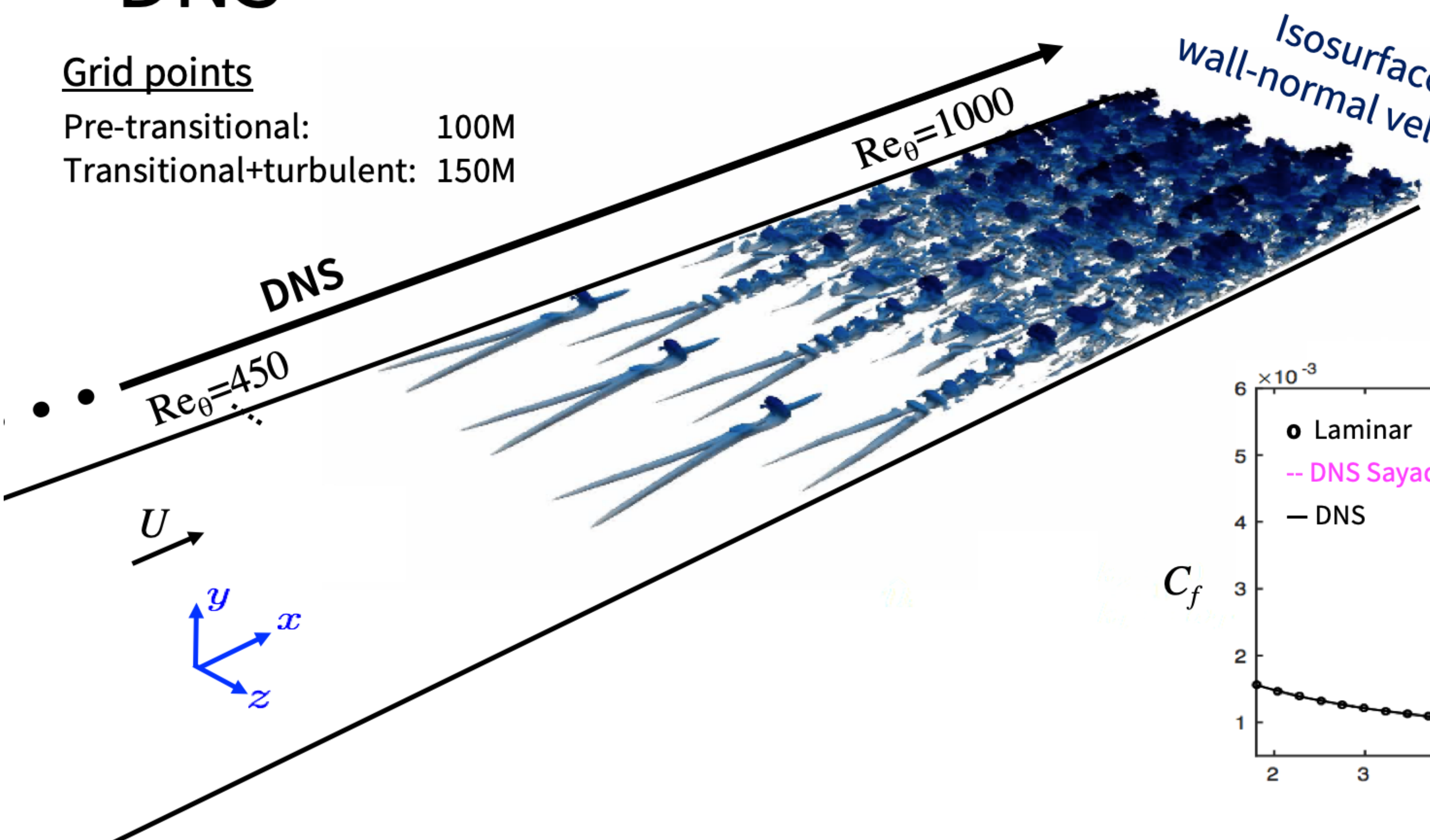

Friction Coefficient

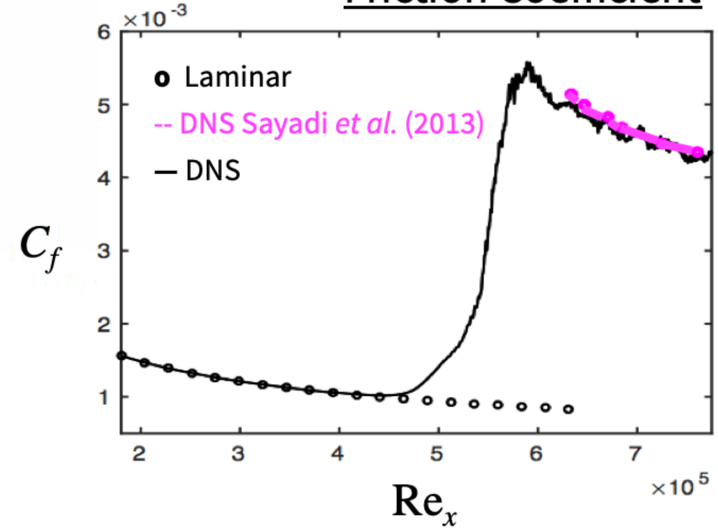

Numerical experiments

Considered setups

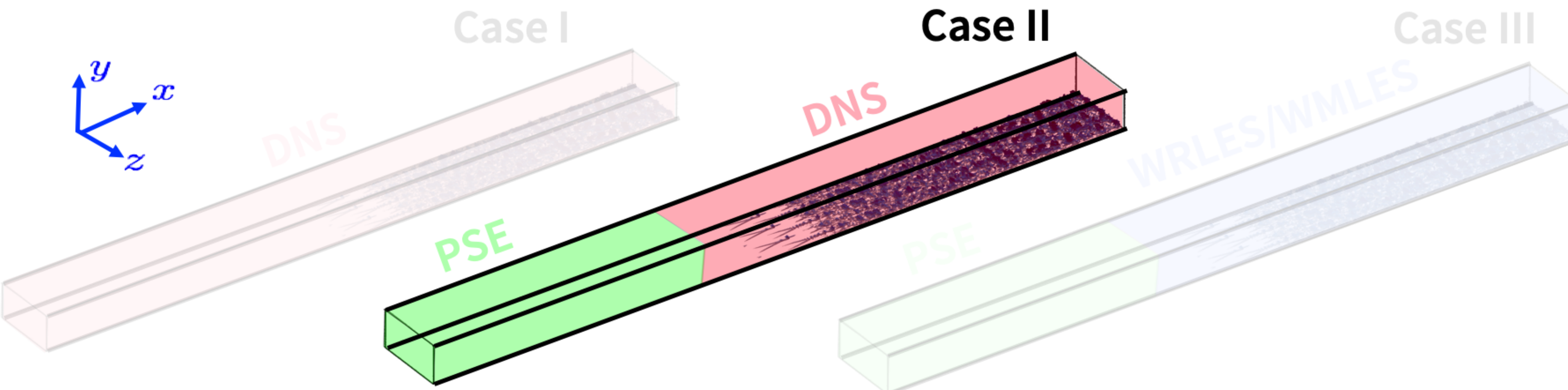

PSE	DNS	
$\Delta x/\delta_0 = 0.3$	$\Delta x/\delta_0 = 0.05$	$\Delta x^+ = 7.2$
$\Delta y_{\min}/\delta_0 = 0.001$	$\Delta y_{\min}/\delta_0 = 0.003$	$\Delta y^+_{\min} = 0.3$
7 Fourier modes in z	$\Delta z/\delta_0 = 0.03$	$\Delta z^+ = 5.1$

PSE+DNS

<u>Grid points</u>

Pre-transitional:	**0.2M (↓ 99.8%)**
Transitional+turbulent:	150M

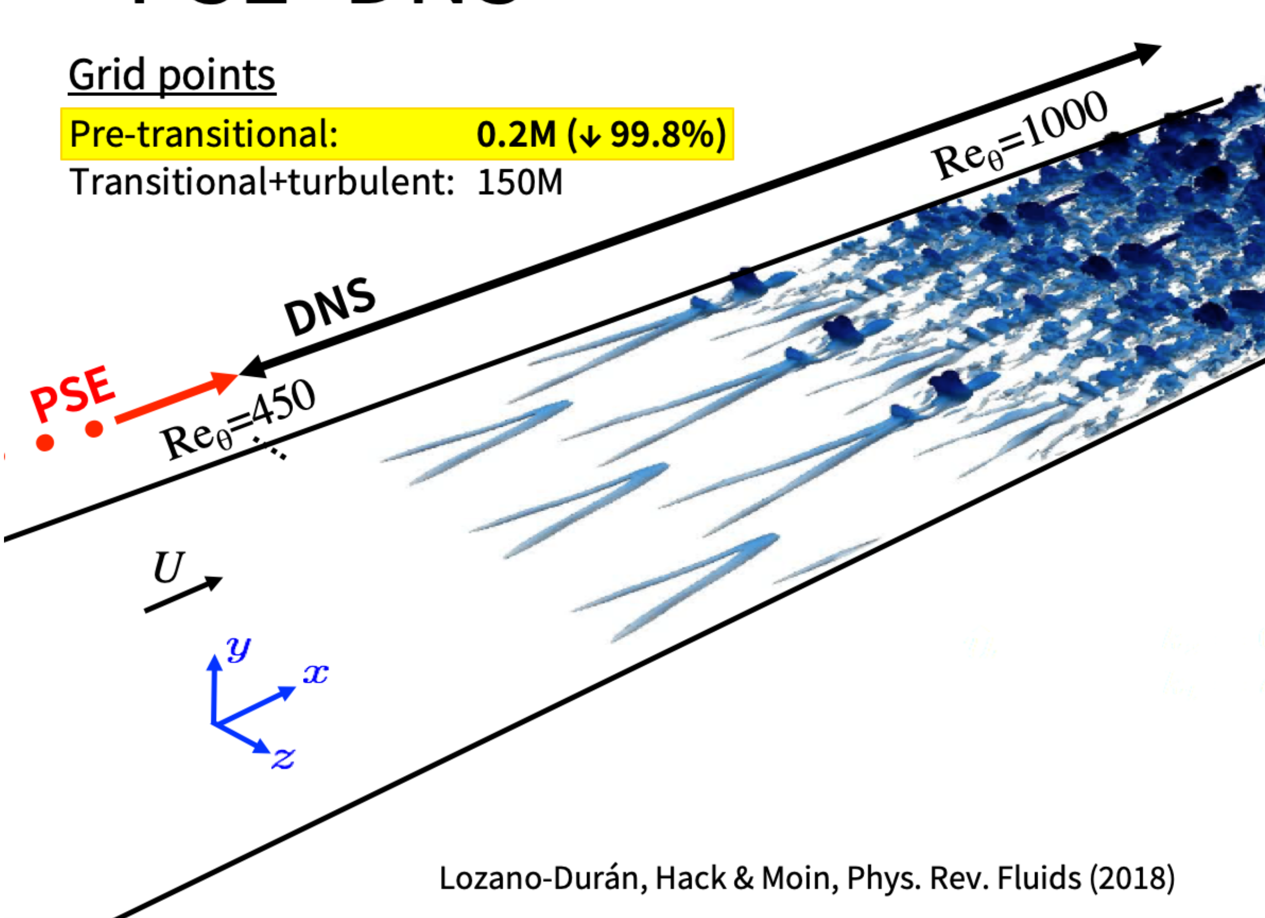

<u>Friction Coefficient</u>

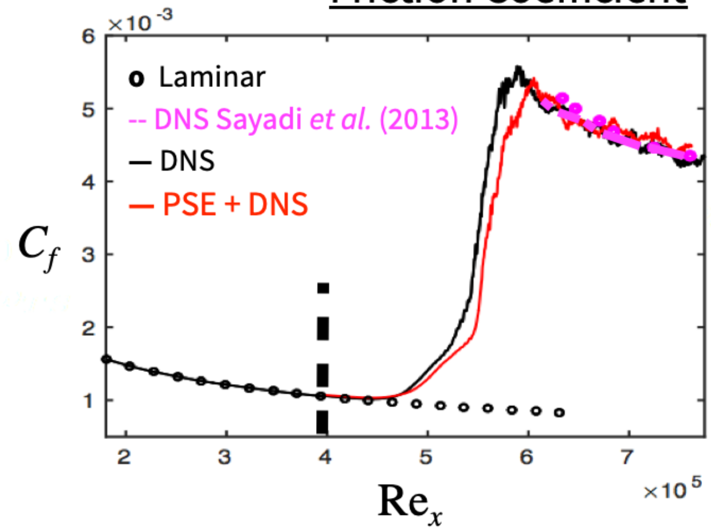

Lozano-Durán, Hack & Moin, Phys. Rev. Fluids (2018)

Pre-transitional region

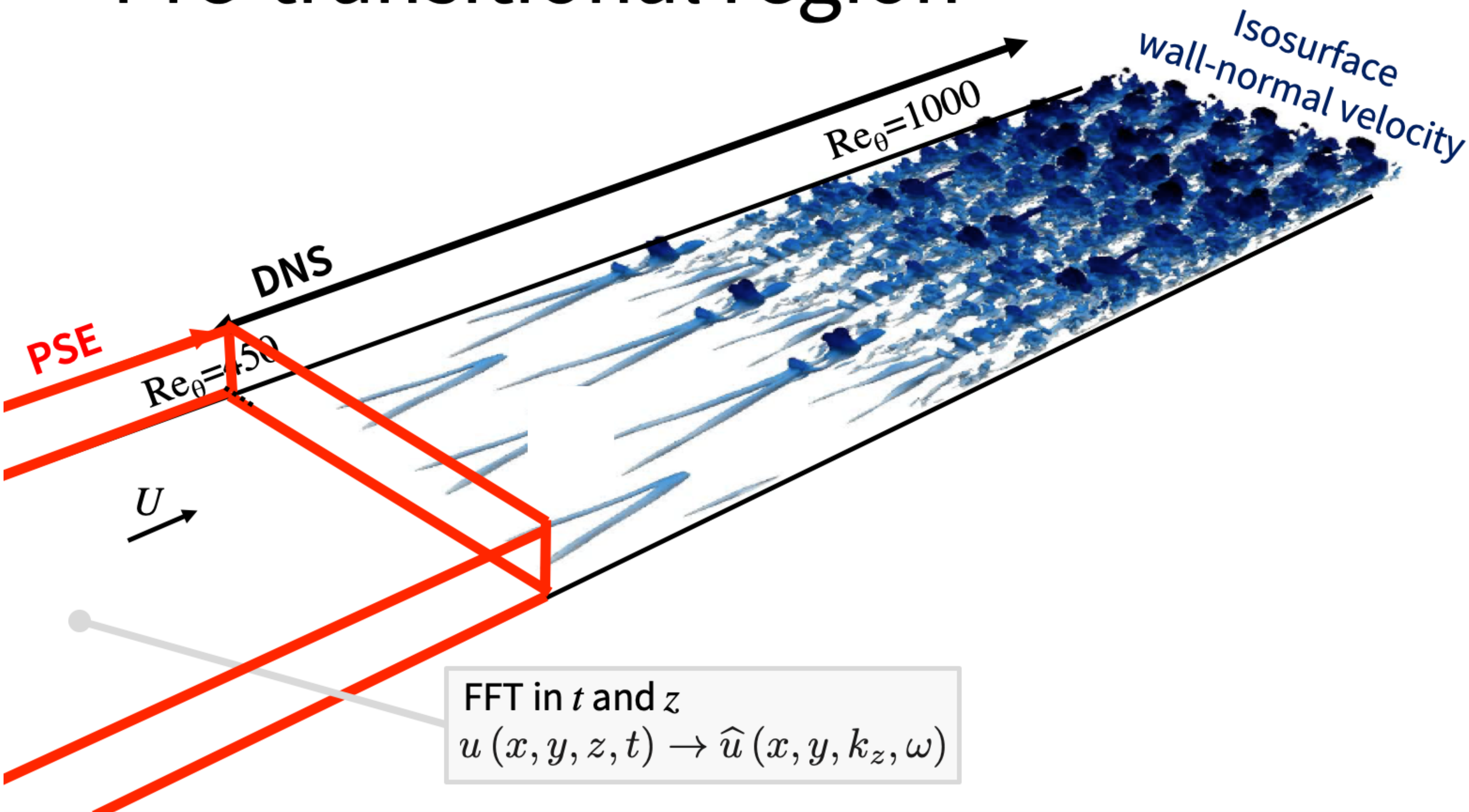

Stanford

Pre-transitional region

→ *accurately captured by the PSE*

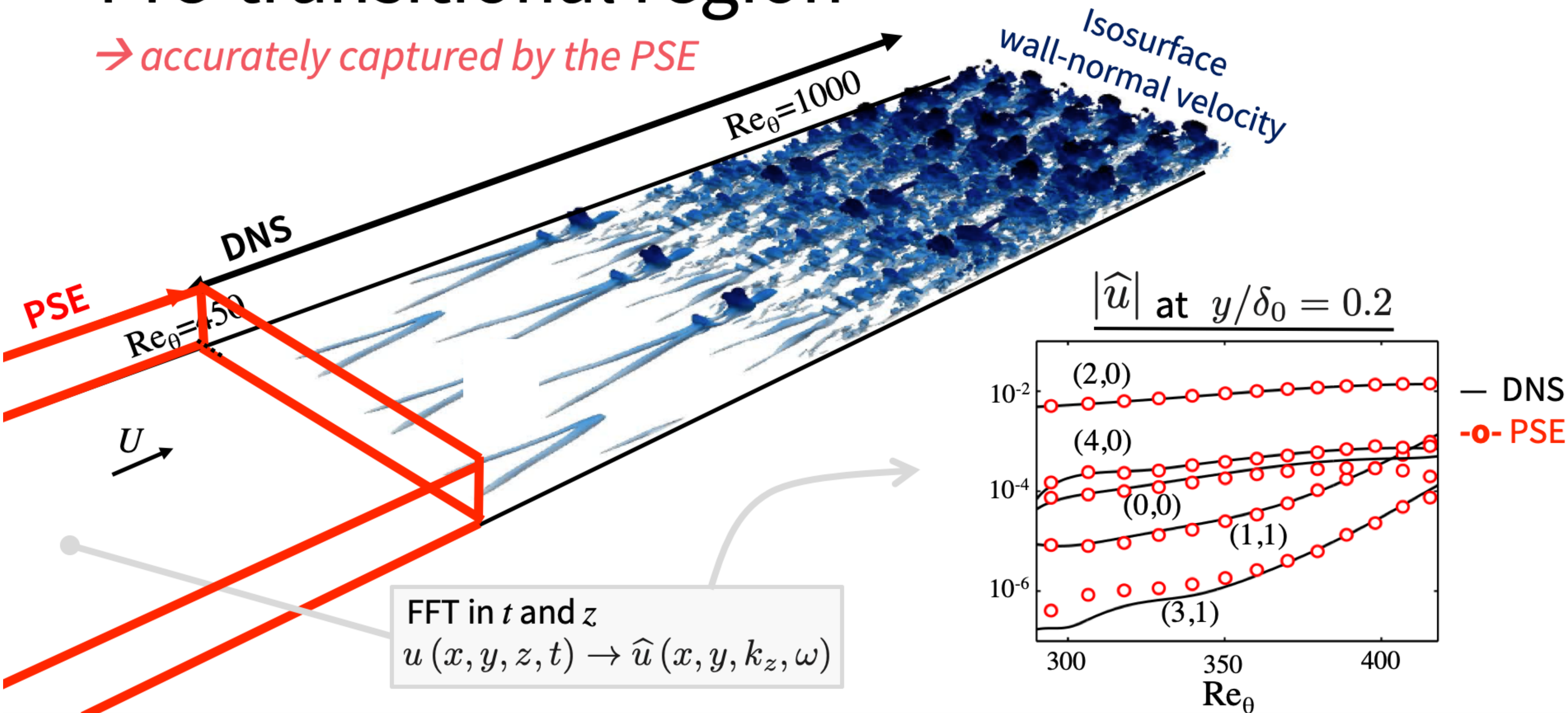

Pre-transitional region

Flow structure

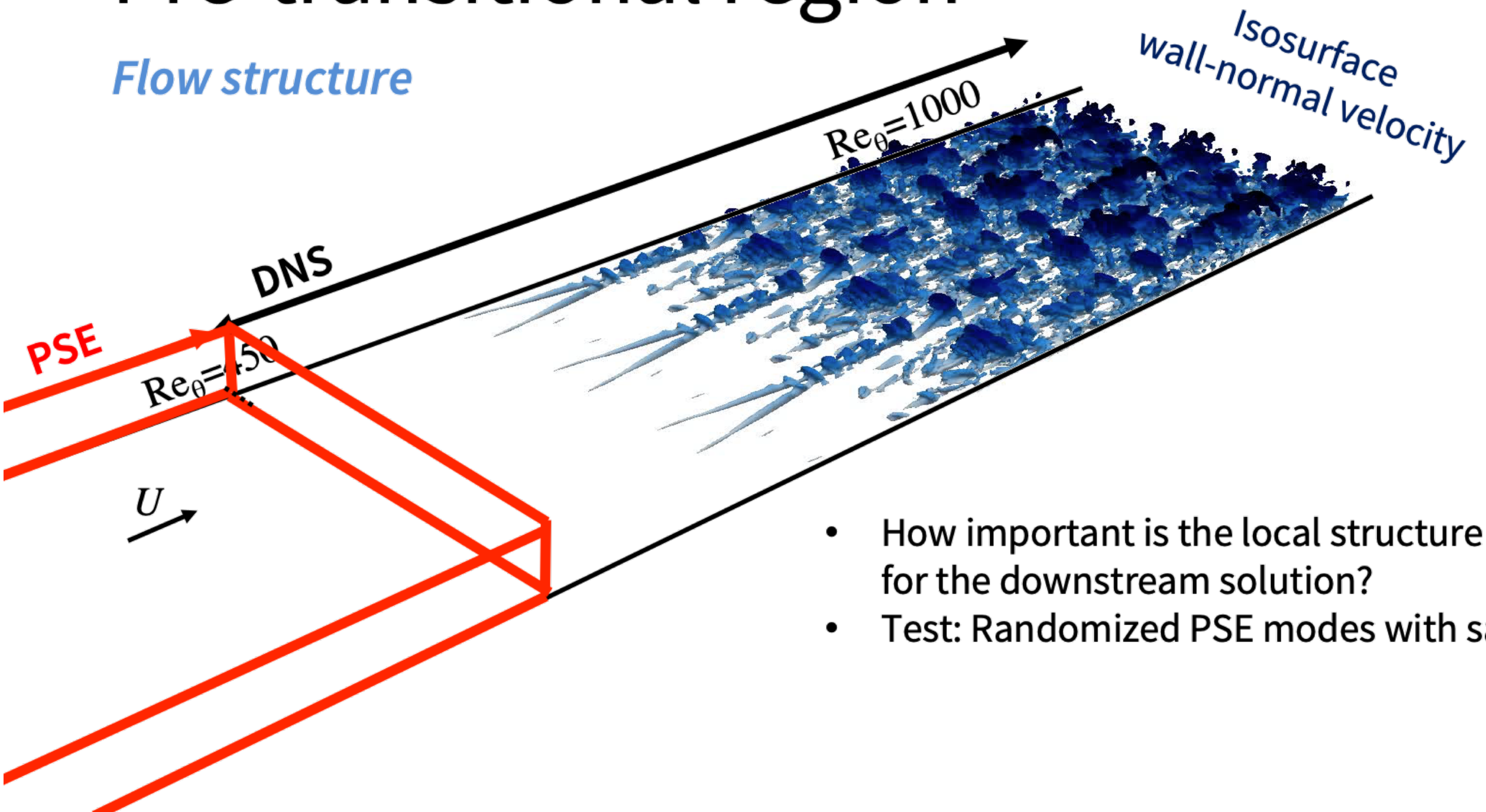

- How important is the local structure of the flow for the downstream solution?
- Test: Randomized PSE modes with same total energy

Stanford

Pre-transitional region

Flow structure

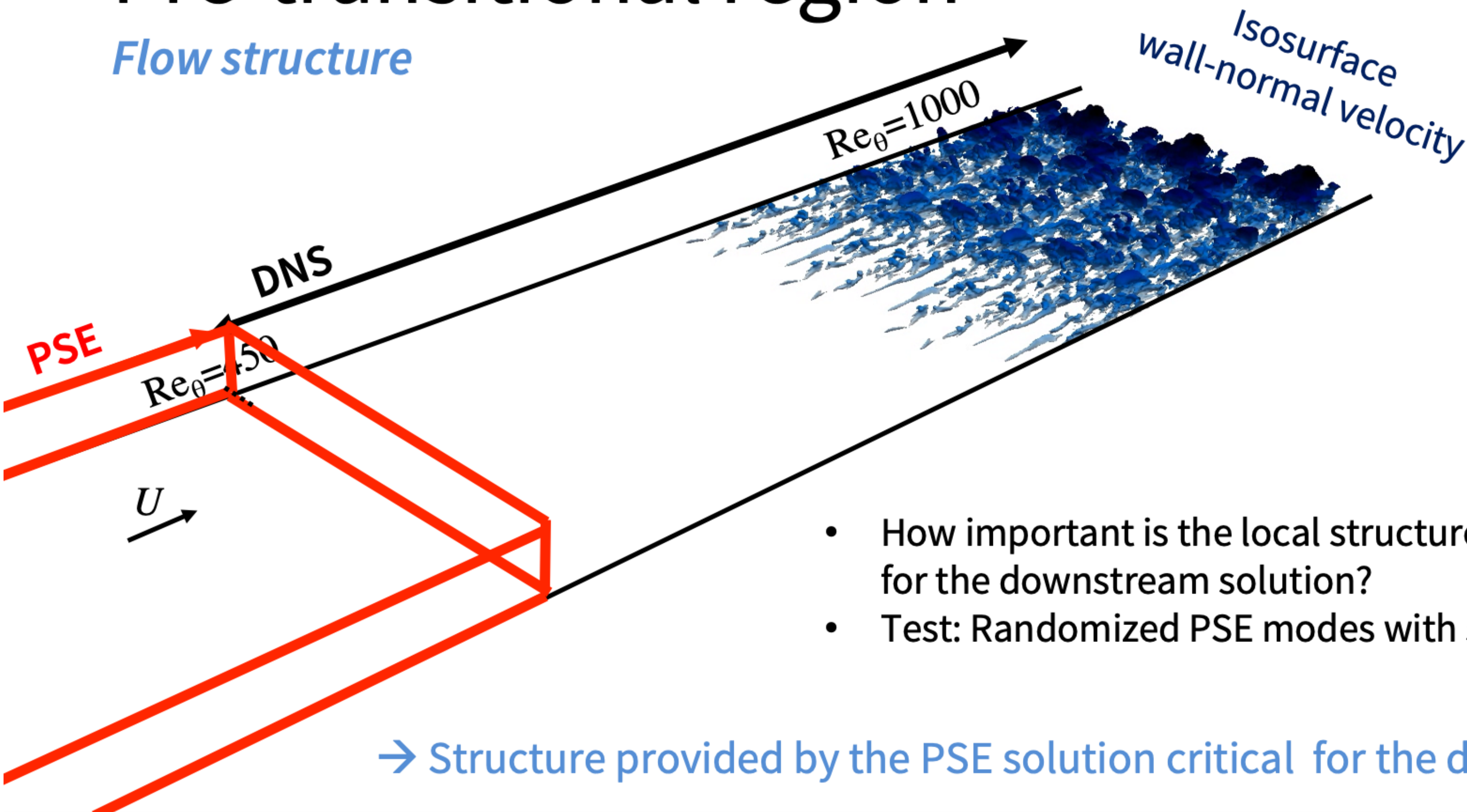

- How important is the local structure of the flow for the downstream solution?
- Test: Randomized PSE modes with same total energy

→ Structure provided by the PSE solution critical for the downstream flow

Turbulent region

Flow statistics

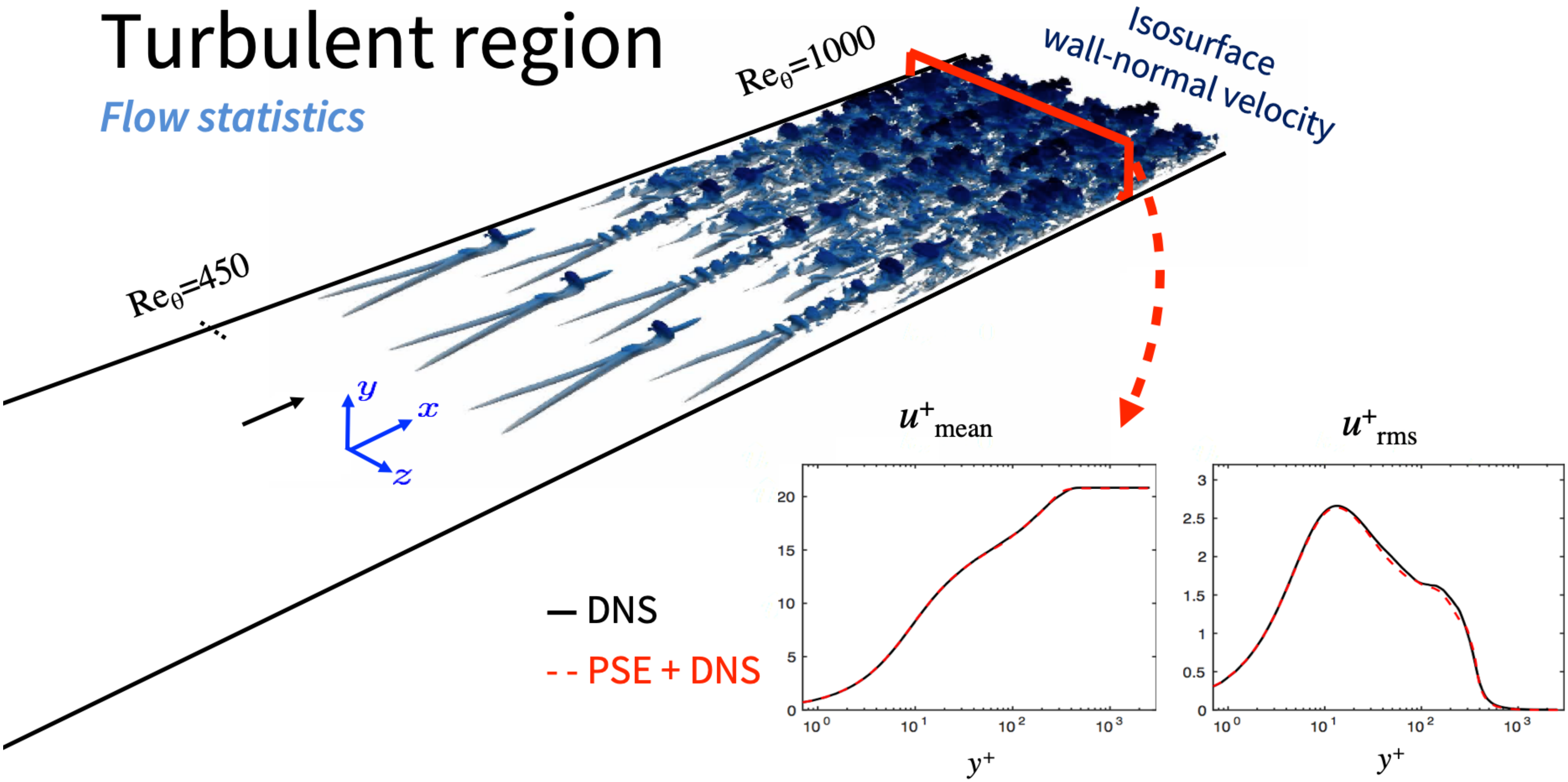

Numerical experiments

Considered setups

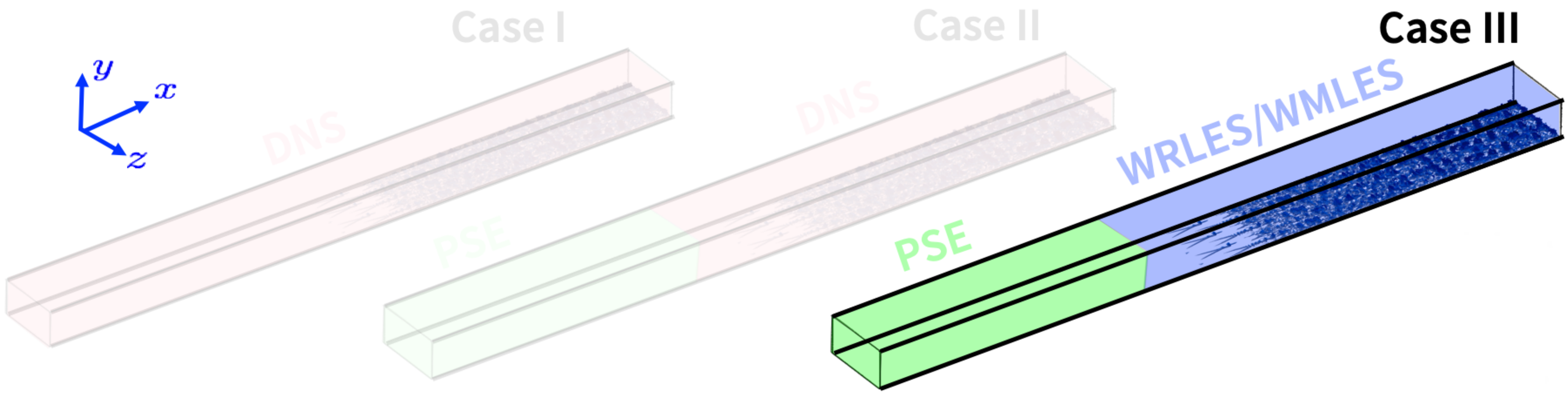

PSE	WRLES		WMLES
$\Delta x/\delta_0 = 0.3$	$\Delta x/\delta_0 = 0.31$	$\Delta x^+ = 45$	$\Delta x^+ = 45$
$\Delta y_{\min}/\delta_0 = 0.001$	$\Delta y_{\min} = 0.010$	$\Delta y^+_{\min} = 1$	$\Delta y^+_{\min} = 18$
7 Fourier modes in z	$\Delta z/\delta_0 = 0.13$	$\Delta z^+ = 22$	$\Delta z^+ = 22$

Large-eddy simulation

- ## Dynamic Smagorinsky SGS model

Germano et al., Phys. Fluids 1991; Lilly, Phys. Fluids 1992

SGS stress closure:

$$\tau_{ij} - \frac{1}{3}\delta_{ij}\tau_{kk} = 2C\Delta^2|\bar{S}|\bar{S}_{ij}$$

based on large-scale strain $\bar{S}_{ij} = \frac{1}{2}\left(\frac{\partial \bar{u}_i}{\partial x_j} + \frac{\partial \bar{u}_j}{\partial x_i}\right)$

with Smagorinsky coefficient

$$C = \frac{1}{2}\left(L_{ij}M_{ij}/M_{ij}^2\right)$$

using the resolved turbulent stress

$$L_{ij} = -\widehat{u_i u_j} + \hat{\bar{u}}_i \hat{\bar{u}}_j$$

and $M_{ij} = \widehat{\Delta^2}|\hat{\bar{S}}|\hat{\bar{S}}_{ij} - \Delta^2\widehat{|\bar{S}|\bar{S}_{ij}}$

- ## Equilibrium wall model

Kawai & Larsson, Phys. Fluids 2012

Solution of ODE near wall: $\frac{d}{dn}\left[(\mu + \mu_R)\frac{dU}{dn}\right] = 0$

with eddy viscosity μ_R taken from mixing-length hypothesis

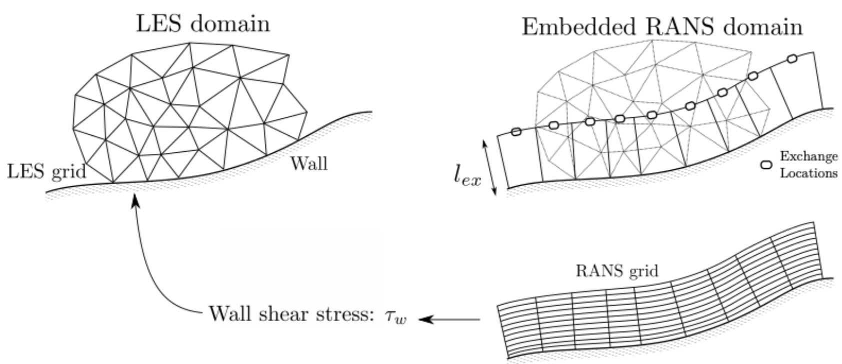

DNS

<u>Grid points</u>

Pre-transitional: 100M
Transitional+turbulent: 150M

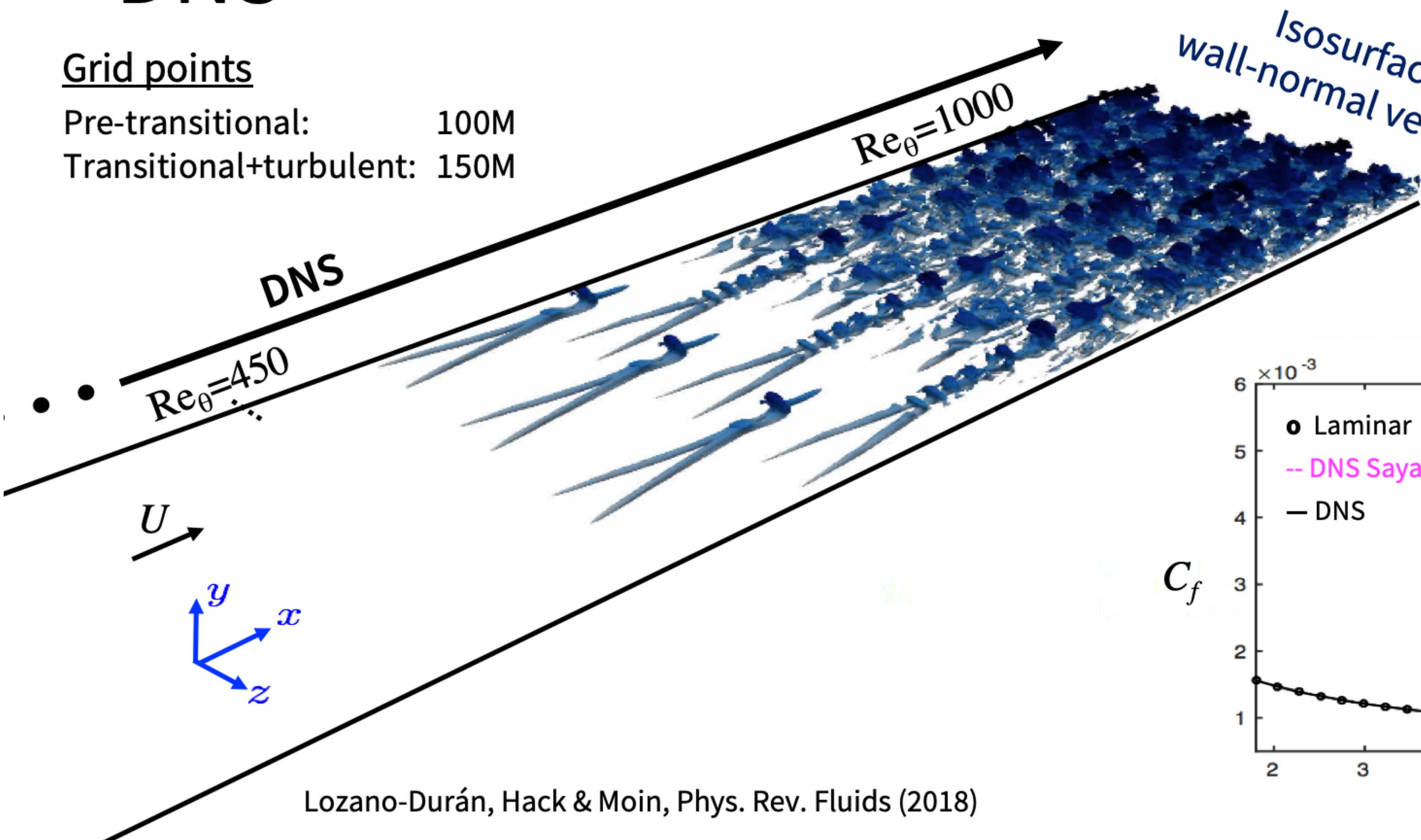

Lozano-Durán, Hack & Moin, Phys. Rev. Fluids (2018)

<u>Friction Coefficient</u>

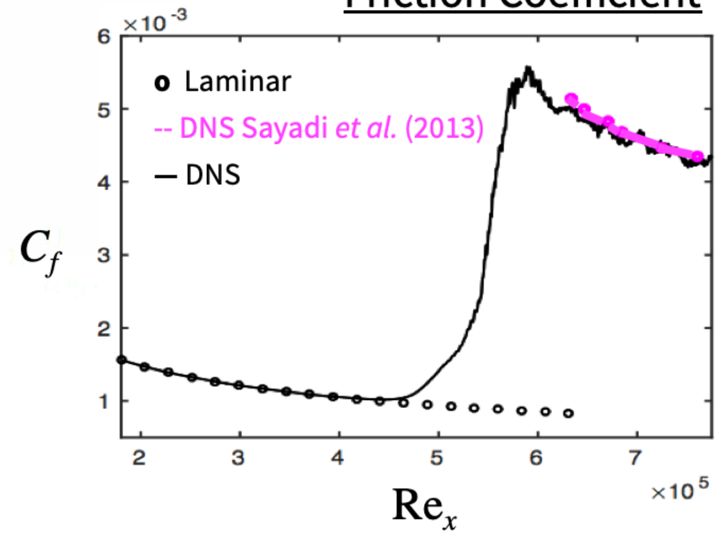

PSE+WRLES

Grid points

Pre-transcritional: 0.2M (↓ **99.8%**)
Transitional+turbulent: 4M (↓ **98.4%**)

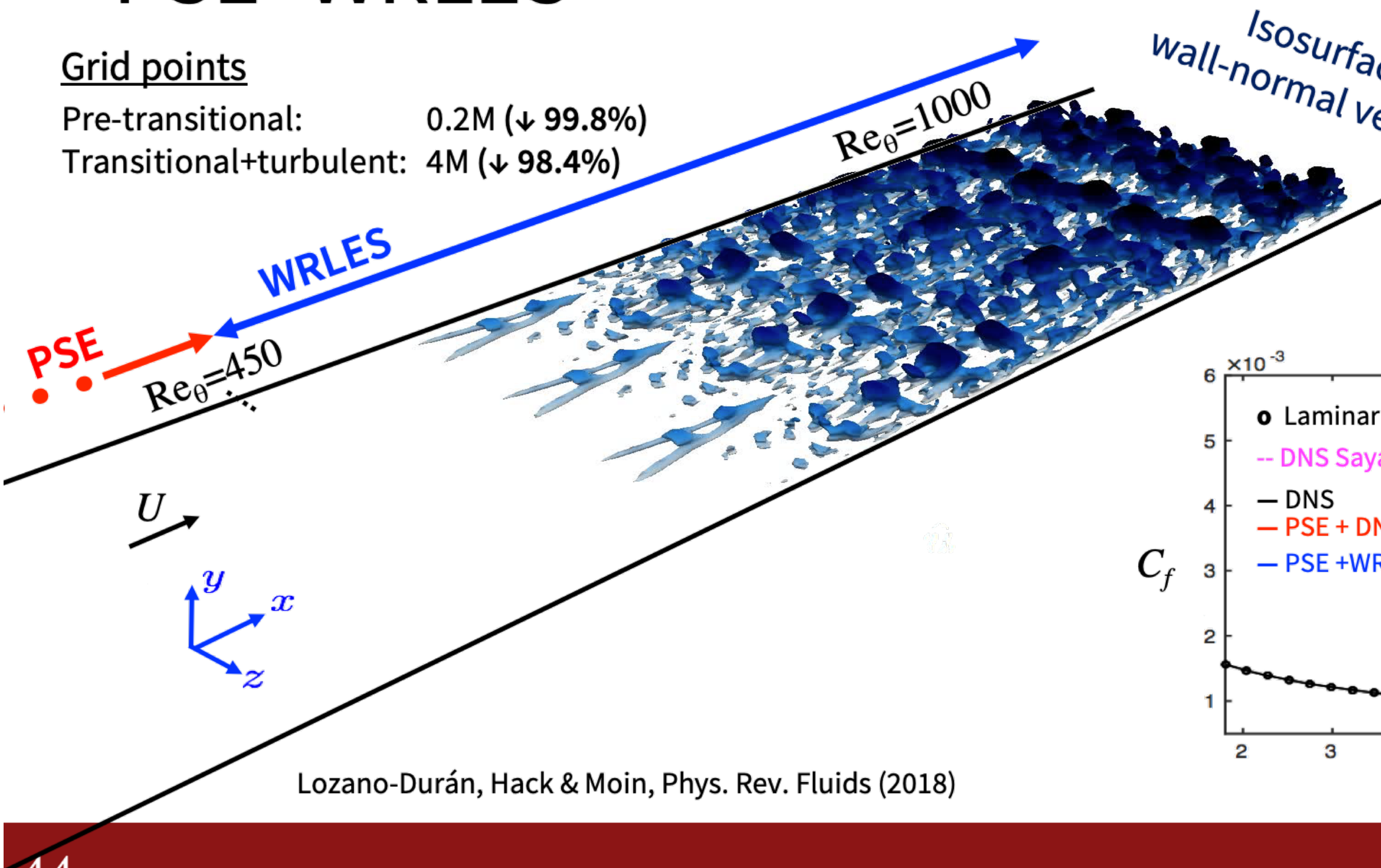

Lozano-Durán, Hack & Moin, Phys. Rev. Fluids (2018)

Friction Coefficient

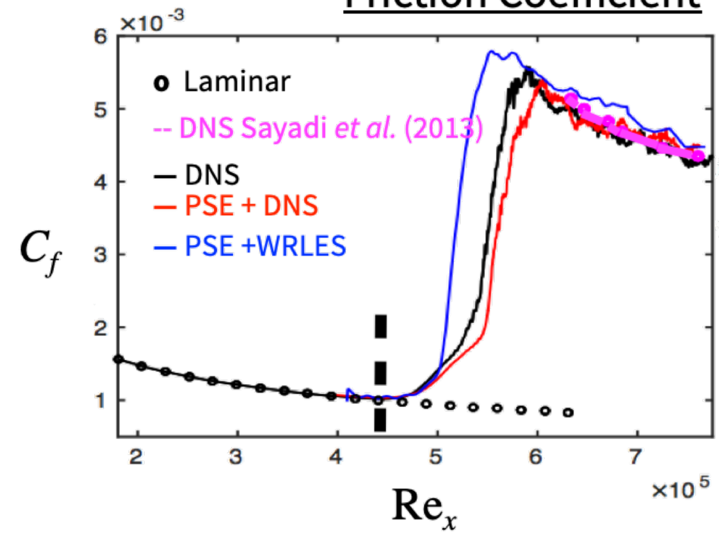

Stanford

PSE+WMLES

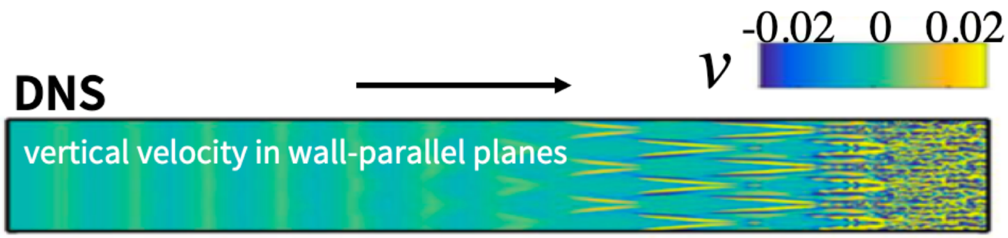

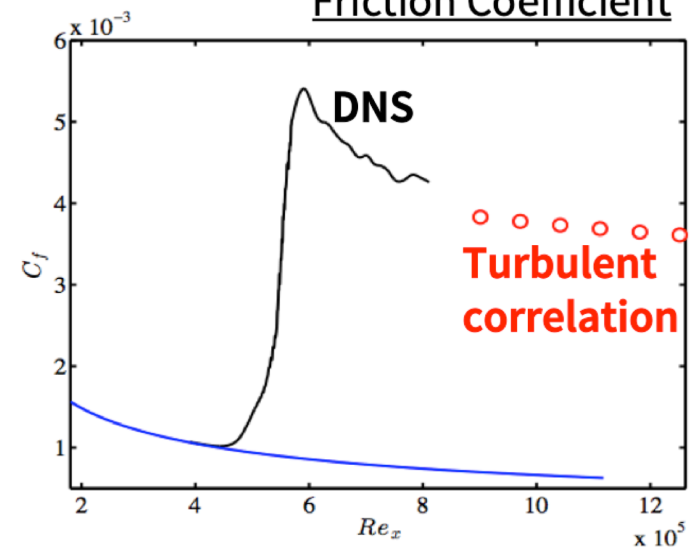

Lozano-Durán, Hack & Moin, Phys. Rev. Fluids (2018)

PSE+WMLES

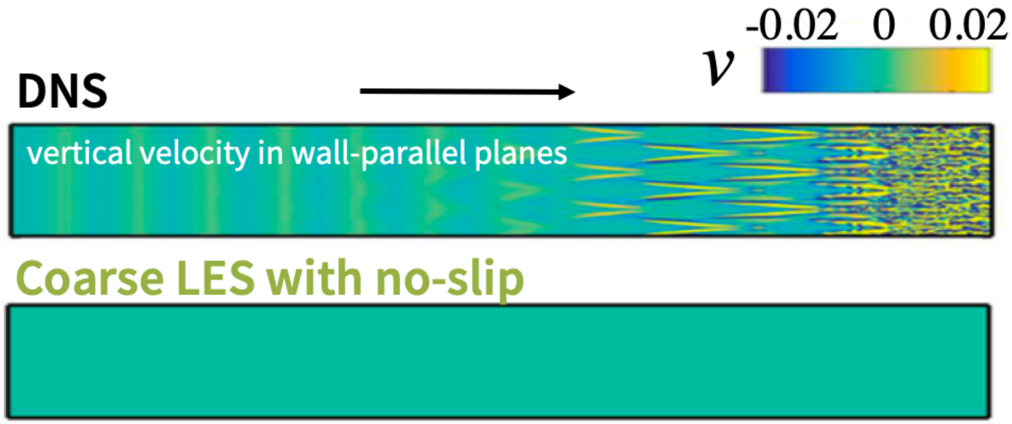

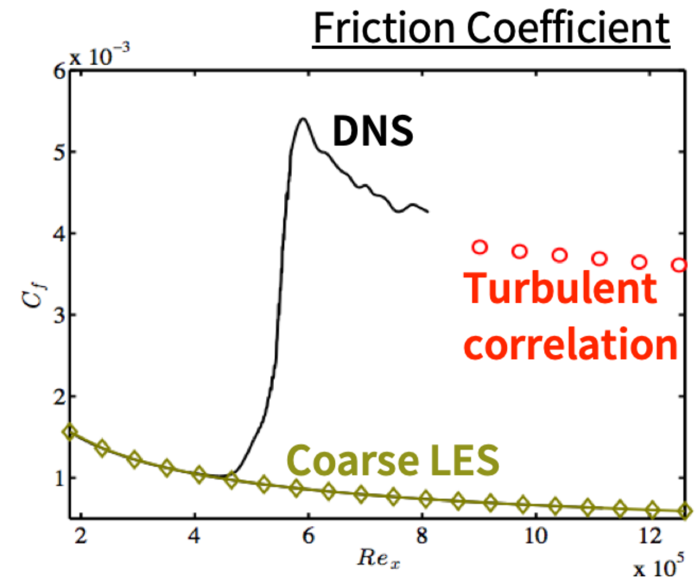

Lozano-Durán, Hack & Moin, Phys. Rev. Fluids (2018)

PSE+WMLES

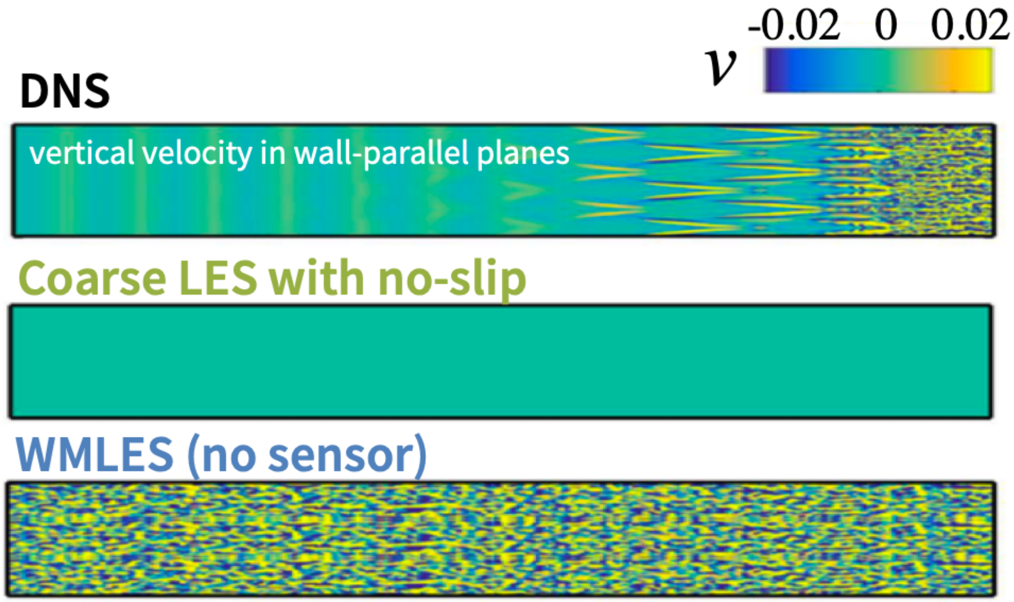

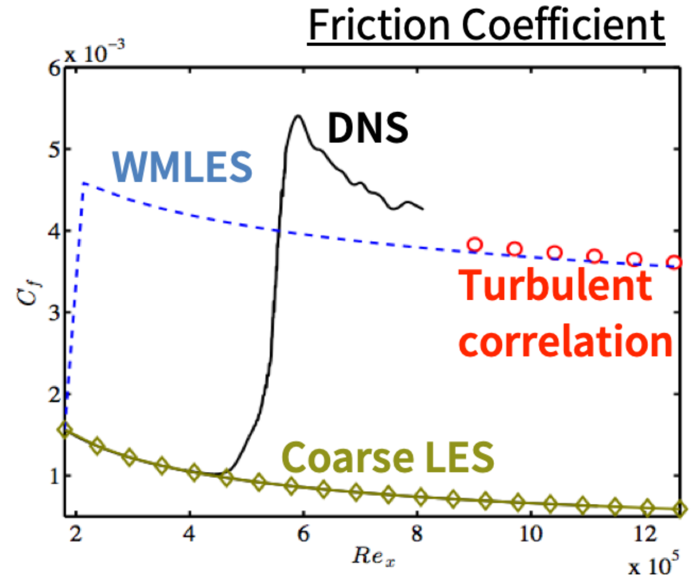

Lozano-Durán, Hack & Moin, Phys. Rev. Fluids (2018)

PSE+WMLES

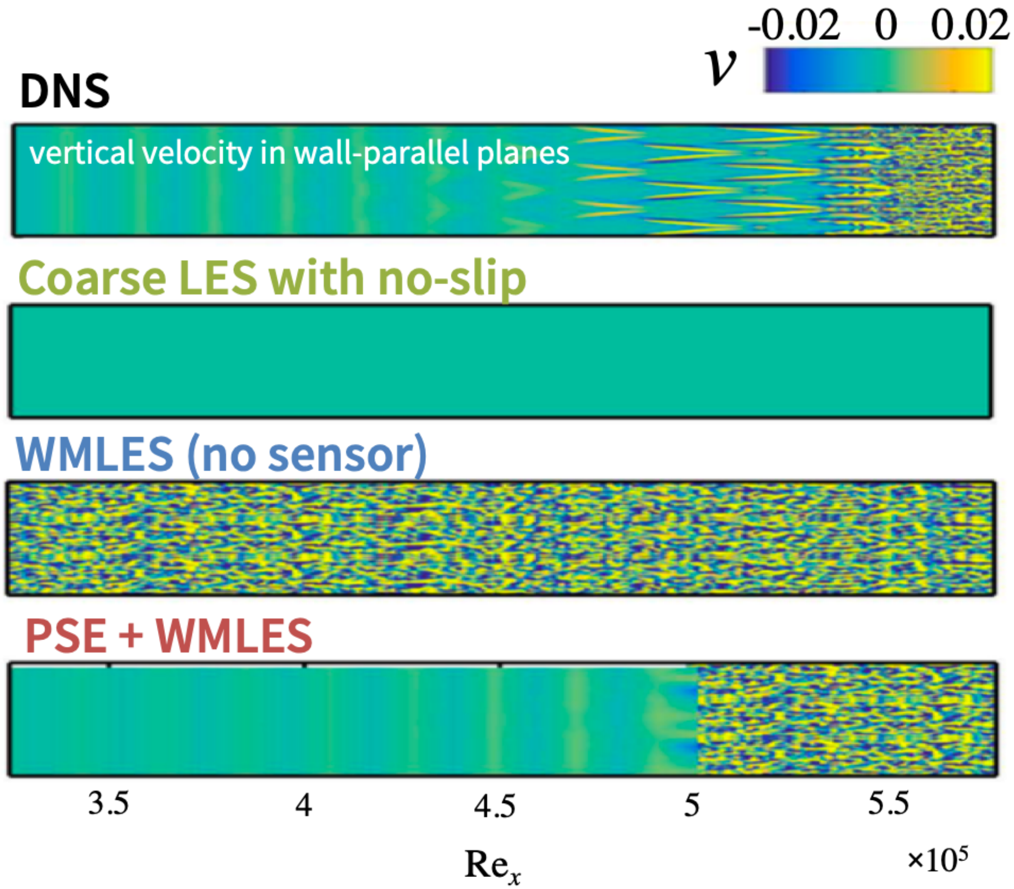

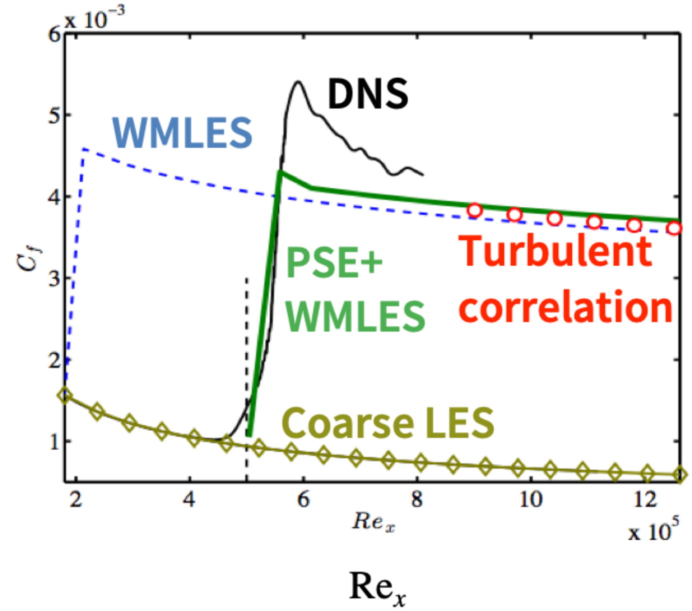

Lozano-Durán, Hack & Moin, Phys. Rev. Fluids (2018)

Stanford

Turbulent region

Flow statistics

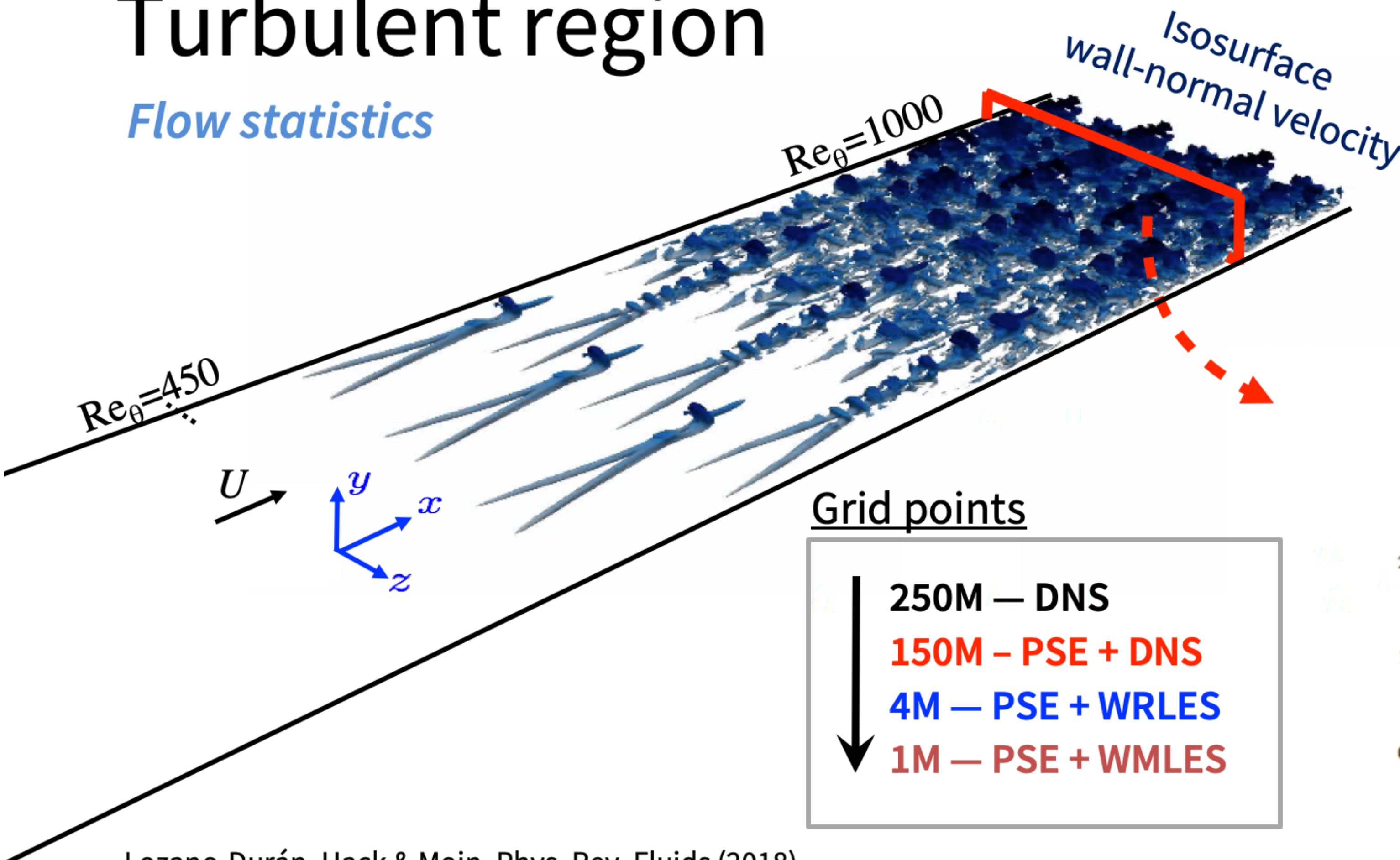

Grid points

250M — DNS
150M – PSE + DNS
4M — PSE + WRLES
1M — PSE + WMLES

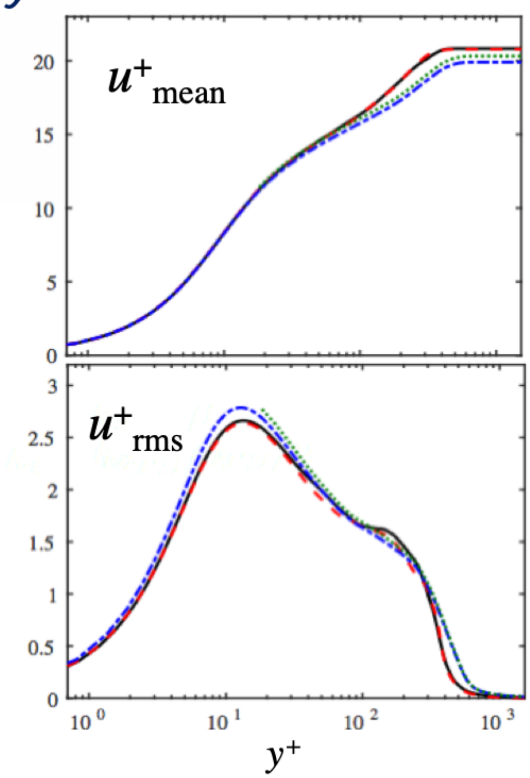

Lozano-Durán, Hack & Moin, Phys. Rev. Fluids (2018)

Transition scenarios

NATURAL

- Low levels of external disturbances
- Exponential amplification of primary disturbances (TS waves)
- Classical configurations: H/K-type (Herbert 1988, Kachanov 1984)

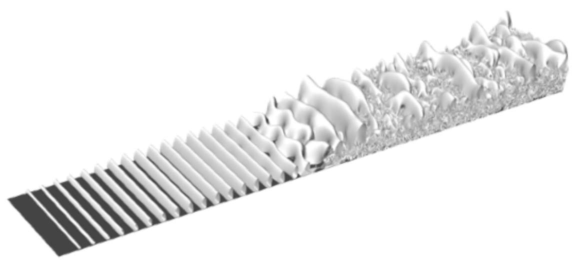

BYPASS

- Moderate levels of external disturbances
- Algebraic amplification of primary disturbances (streaks)
- Exponential secondary instability

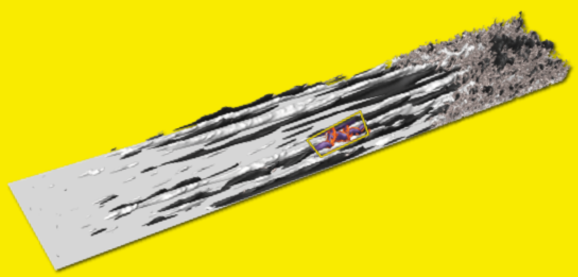

CROSSFLOW

- Inflectional (exponential) primary disturbance
- Rapid breakdown to turbulence

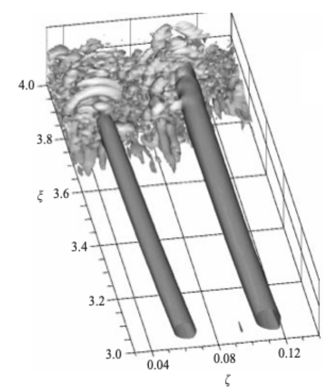

Bypass transition

- Faster path to turbulence than transition via Tollmien-Schlichting waves
- Observed in boundary layers exposed to free-stream turbulence (turbo machinery)
- Mediated by the formation of highly energetic streaks inside the boundary layer
- Capturing the mean flow distortion is essential to predict bypass transition

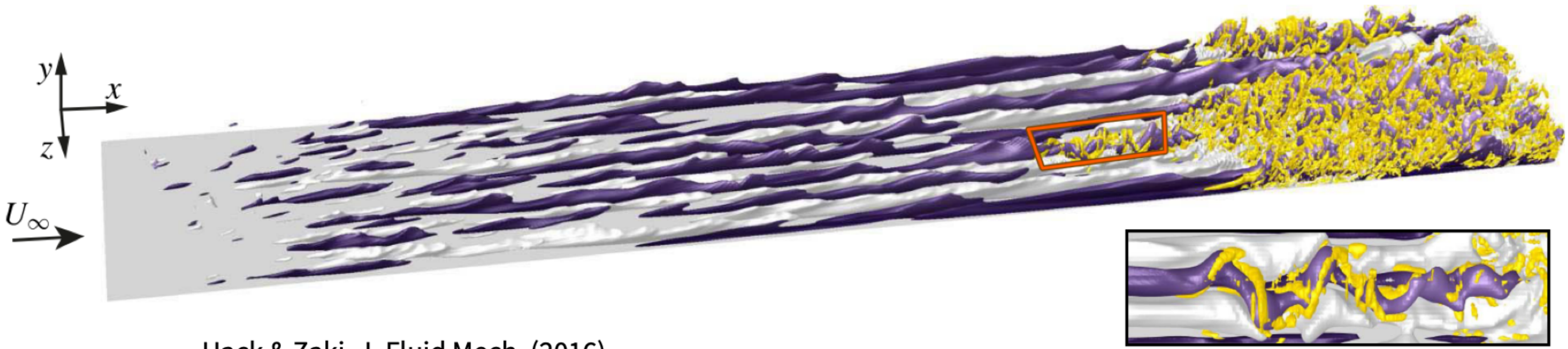

Hack & Zaki, J. Fluid Mech. (2016)

Streak formation via lift-up

Streaks are the outcome of the displacement of the mean momentum of the boundary layer by wall-normal perturbations *(Landahl 1975)*

- Ejections lead to low-speed streaks near the edge of the boundary layer
- Sweeps produce high-speed streaks near the wall

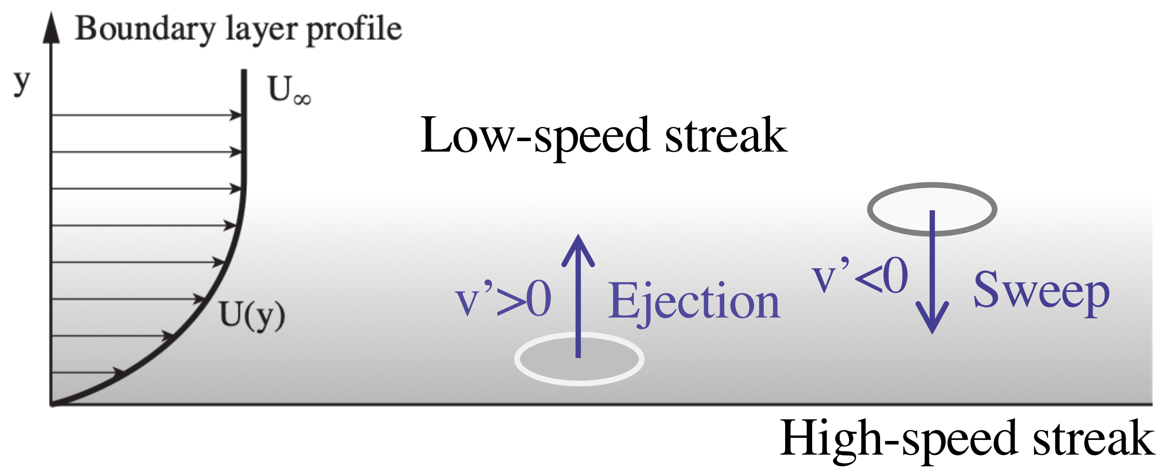

Model problem: periodic streaks

<u>Upstream perturbation: counter-rotating vortices</u>

Vector v’, w’ — cross-section

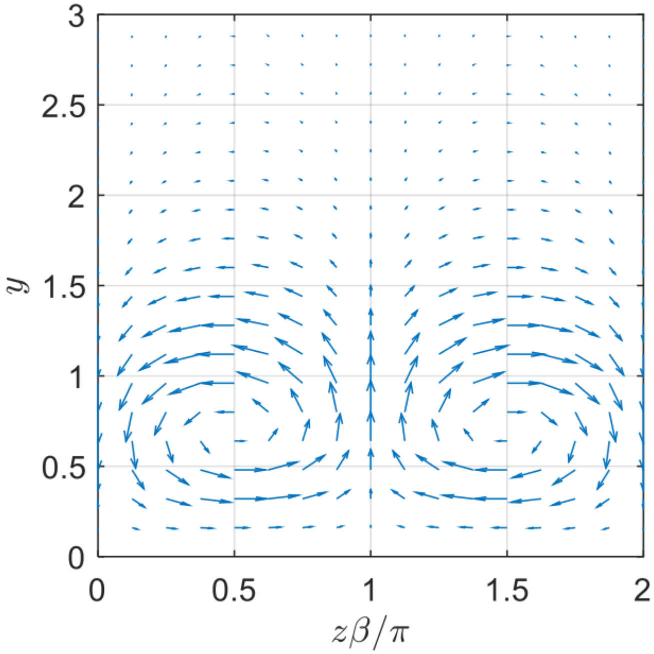

<u>Flow response: streaks</u>

Isosurfaces u’ — top view

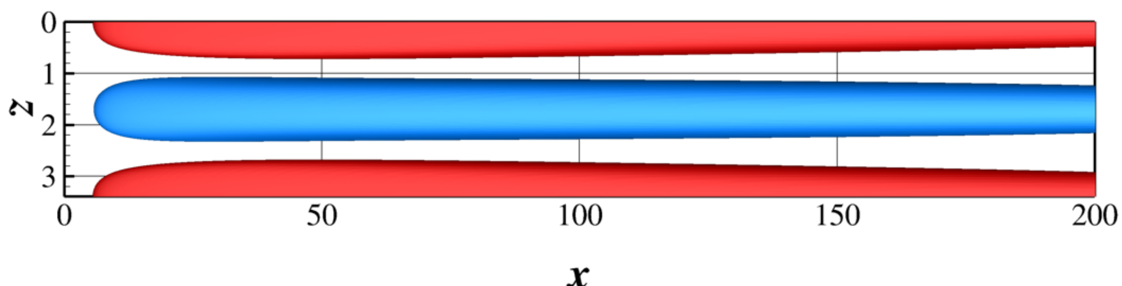

→ Transient growth generates streaks

Mean-flow distortion

Low-amplitude (linear) streaks:

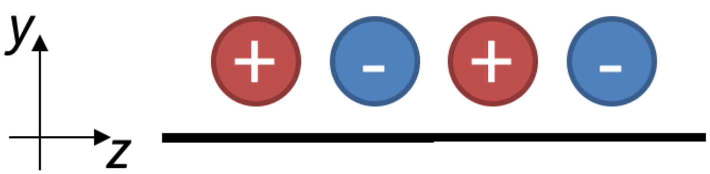

Mean-flow distortion

Low-amplitude (linear) streaks:

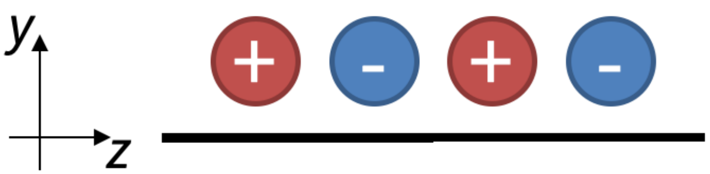

High-amplitude (nonlinear) streaks:

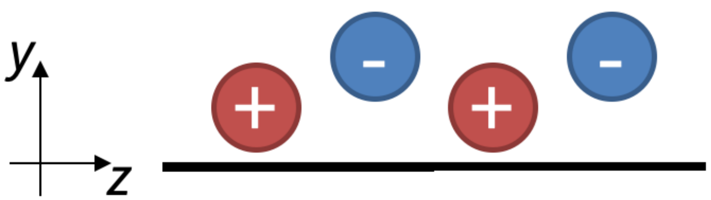

Mean-flow distortion

Low-amplitude (linear) streaks:

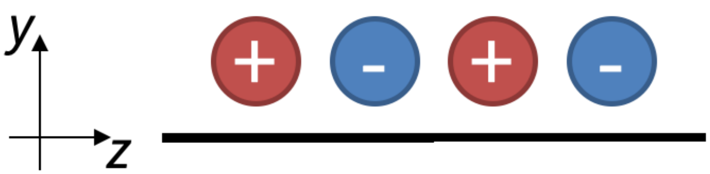

High-amplitude (nonlinear) streaks:

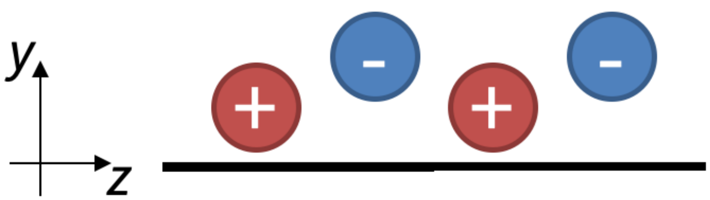

Mean flow distortion

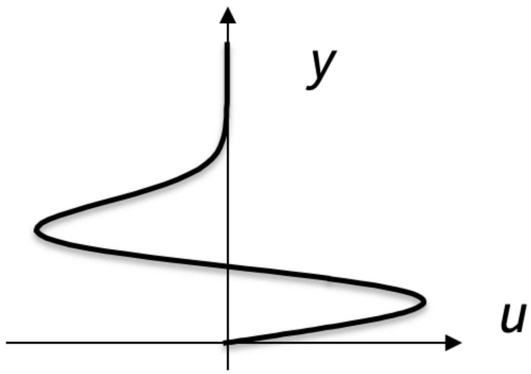

→ High-amplitude streaks modify the mean shear of the boundary layer
→ Critically affects the amplification of secondary instabilities

Mean-flow distortion with PSE

In classical PSE, Mean Flow Distortion (MFD) is handled as a (β=0,ω=0) instability mode and added to the Blasius solution

$$Re_{\delta_{\mathrm{blas}}} = 162 \qquad \max\left(\|u\|\right) = 0.0373$$

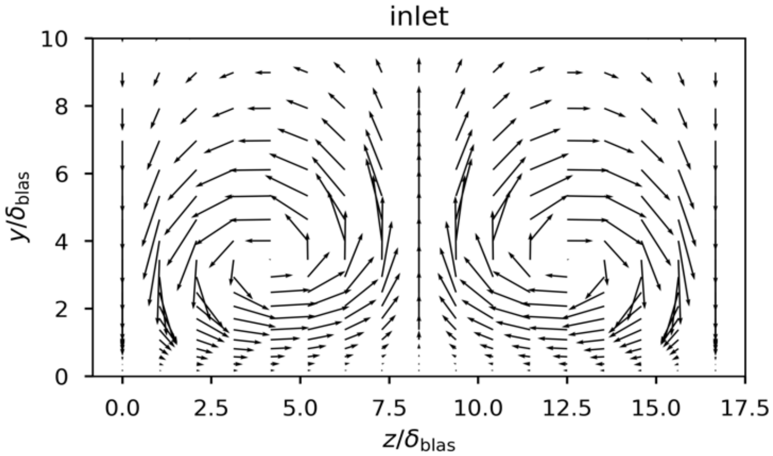

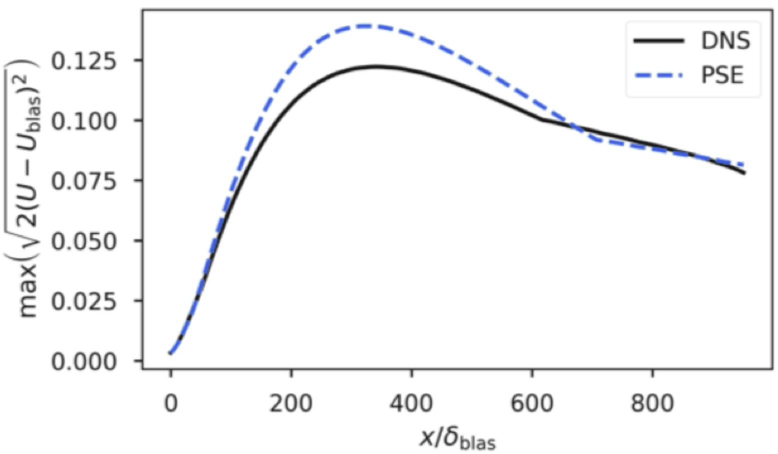

→ PSE computation of mean-flow distortion fails for high amplitudes

Spatial Perturbation Equations (SPE)

- New framework for computing the spatial evolution of nonlinear perturbations
- In the SPE, the base flow is computed by marching the boundary layer equations

Classic boundary layer equations

$$\frac{\partial \bar{u}}{\partial x} + \frac{\partial \bar{v}}{\partial y} = 0$$

$$\bar{u}\frac{\partial \bar{u}}{\partial x} + \bar{v}\frac{\partial \bar{u}}{\partial y} + \frac{1}{\rho}\frac{\partial \bar{P}}{\partial x} - \nu\left(\frac{\partial^2 \bar{u}}{\partial y^2}\right) = 0$$

$$\frac{1}{\rho}\frac{\partial \bar{P}}{\partial y} = 0$$

Spatial Perturbation Equations (SPE)

- New framework for computing the spatial evolution of nonlinear perturbations
- In the SPE, the base flow is computed by marching the boundary layer equations
- Addition of forcing terms (averaged nonlinear terms) introduces MFD into the base flow

Classic boundary layer equations MFD forcing terms

$$\frac{\partial \bar{u}}{\partial x} + \frac{\partial \bar{v}}{\partial y} = 0$$

$$\bar{u}\frac{\partial \bar{u}}{\partial x} + \bar{v}\frac{\partial \bar{u}}{\partial y} + \frac{1}{\rho}\frac{\partial \bar{P}}{\partial x} - \nu\left(\frac{\partial^2 \bar{u}}{\partial y^2}\right) = -\left\langle u_j' \frac{\partial u'}{\partial x_j}\right\rangle$$

$$\frac{1}{\rho}\frac{\partial \bar{P}}{\partial y} = -\left\langle u_j' \frac{\partial v'}{\partial x_j}\right\rangle$$

→ Base flow with MFD obtained from streamwise marching procedure

SPE mean flow distortion

$Re_{\delta_{\rm blas}} = 162$ $\quad\quad$ $\mathrm{x}\,(\|u\|) = 0.0373$

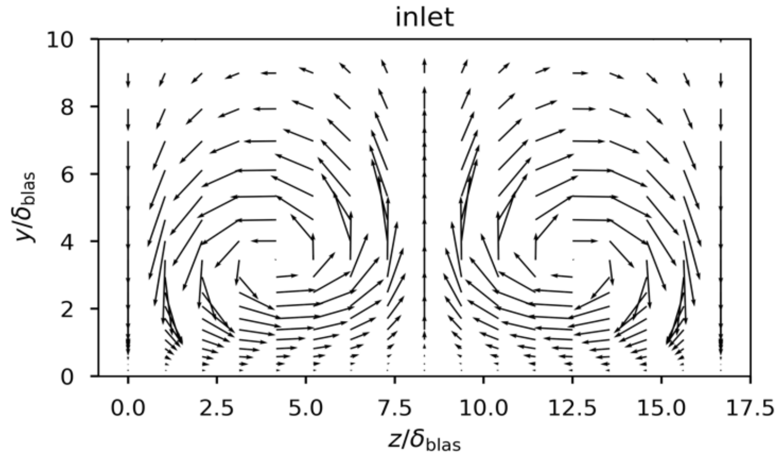

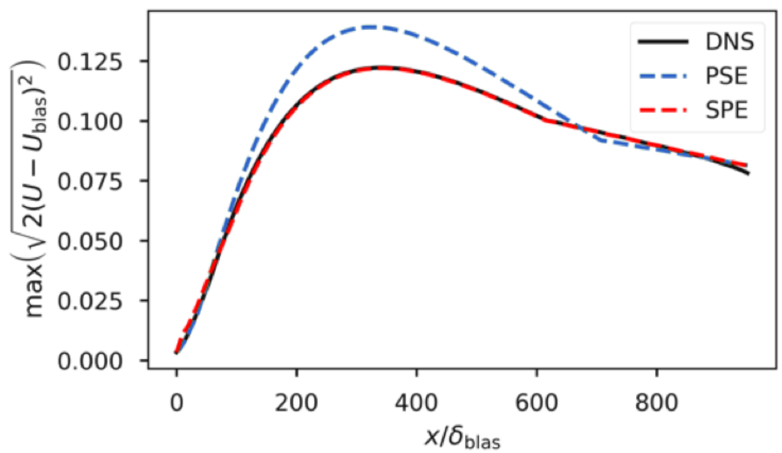

→ SPE captures mean-flow distortion accurately

→ Prerequisite for computing bypass transition

Stanford

Conclusions

- Parabolized stability equations (PSE) provide an accurate representation of the pre-transitional region including
  - Accurate identification of onset of transition
  - Capturing of growth of individual harmonics
  - Substantial computational savings: from 100M to 0.2M points in pre-transitional regime
  - Combination with WMLES reduces computational cost by factor of 250 compared to DNS
- Computation of bypass transition and accurate capturing of mean-flow distortion poses challenges
- Novel SPE framework computes mean-flow distortion as part of the base flow